Pergamon

Prog. Polym. Sci., Vol. 22, 49–92, 1997

0079–6700/97 $32.00

PII: S0079–6700(96)00004–4

THE ZERO AVERAGE CONTRAST CONDITION: THEORETICAL PREDICTIONS AND EXPERIMENTAL EXAMPLES*

MUSTAPHA BENMOUNA[a,b] and BOUALEM HAMMOUDA[c]

[a]*Max-Planck-Institut für Polymerforschung, Postfach 3148, D-55021 Mainz, Germany*
[b]*Permanent address: University of Tlemcen, Institute of Sciences and Technology, Department of Physics, Tlemcen BP 119, Algeria*
[c]*National Institute of Standards and Technology, Material Science and Engineering Laboratory, Bldg 235, Room E151, Gaithersburg, MD 20899, U.S.A.*

Abstract – This paper deals with mixtures of homopolymers and copolymers in solvents under the zero average contrast condition. This condition is chosen in order to decouple the correlations due to polymer composition fluctuations from those due to polymer concentration fluctuations. This makes the measurement of these correlations much easier using techniques based on static light scattering, photoncorrelation spectroscopy, small angle neutron scattering, neutron spin echo or X-ray scattering. In the first part of the paper, a simple theoretical framework is developed to present the guidelines for the interpretation of the scattering data. In the second part, some experimental examples are discussed using the scattering techniques mentioned above. Data obtained from various systems involving alike (deuterated and ordinary) homopolymers and diblock copolymers as well as unalike species are considered. An example of mixtures of polyelectrolytes in aqueous solutions is also discussed within the framework of the zero average contrast condition.

CONTENTS

1. Introduction 50
2. Theoretical predictions 52
   2.1. Static scattering 52
      2.1.1. Scattered intensity and structure factors 52
      2.1.2. Ternary mixtures of homopolymer A/homopolymer B/solvent 55
         2.1.2.1. Polymer B isorefractive with the solvent 55
         2.1.2.2. Homopolymers A and B in a solvent under the ZAC 57
      2.1.3. Quaternary mixtures under the ZAC 59
      2.1.4. Solutions of diblock copolymers AB under the ZAC 61
      2.1.5. Critical fluctuations and the scaling behavior under the ZAC 61
      2.1.6 Some remarks on renormalization group theory 63
   2.2. Dynamic scattering properties 65
      2.2.1. Equations of motion 65
      2.2.2. Dynamic scattering functions 67
      2.2.3. Dynamic scattering under the ZAC 68
      2.2.4. Critical slowing down 69
3. Experimental examples 69
   3.1. PS/PMMA/bromobenzene 69

*This paper is dedicated to Professor Z.A. Akcasu on the occasion of his 70th birthday.

3.2. PS/PDMS/solvent 76
3.3. PMMA/PDMS/chloroform 78
3.4. PS/PDMS/PMMA/toluene 79
3.5. d-PS/PS/PVME 80
3.6. d–PDMS/PDMS/D-toluene/toluene 82
3.7. Diblock copolymers of d-PS–PS/d-toluene/toluene 84
3.8. Diblock copolymer PS-PI in DOP 86
3.9. d-DNA/d-TMA/D_2O/H_2O and d-PSS/d-TMA/D_2O/H_2O 87
4. Conclusions 89
Acknowledgements 90
References 90

1. INTRODUCTION

In the last decade, a growing effort has been devoted to the study of structural properties and phase behavior of polymer blends and copolymers in bulk and in solution using X-ray, laser and neutron scattering techniques.[1–4] The chemical nature of polymers involved in the mixture and the type of information one seeks determines the choice of the technique to be used. For example, long range fluctuations and slow dynamics are conveniently probed by light scattering, whereas neutrons and X-rays are more suitable for probing the internal properties of polymers or the ordered structures of their phases and the characteristic motion of chains within these phases. In this paper, we are interested in the properties of polymer mixtures and copolymers in homogeneous single phase states. We will also look into some of the scattering properties governed by critical fluctuations when the mixture, although remaining stable and homogeneous, is driven gradually close to the stability limit. This is the case when the temperature T is close to the critical value T_c where $\varepsilon = |T - T_c|/T$ is very small and the mixture undergoes phase separation.

For a pure blend, if the chemical nature and the molecular weigths M_a and M_b of the two polymers A and B are known, one needs to know the radii of gyration R_{ga} and R_{gb} and the interaction parameter χ_{ab} to achieve a first order characterization of the properties of these polymers. The above scattering techniques are standard tools which deal with this problem.

In the case of multicomponent mixtures, the number of parameters increases quickly with the number of components. Consequently, the interpretation of scattering data becomes more difficult unless one simplifies the analysis by choosing polymers that fulfill special conditions. A typical example is given by a ternary mixture in which a low molecular weight solvent is added to the polymer blend. The easiest way to deal with this problem is to use the pseudo-binary description assuming that the effect of solvent is simply to swell the two polymers but adds no further complication to their properties. In this description, the ternary mixture is considered as a blend of homopolymers A and B which is characterized by an effective contrast factor $(\nu_a - \nu_b)^2_{eff} = \varphi(\nu_a - \nu_b)^2$and an effective interaction parameter $\chi_{eff} = \chi_{ab}\varphi$, where $\nu_a - \nu_b$ represents either the difference of the increments of refractive indices $(\partial n/\partial c_a) - (\partial n/\partial c_b)$ if one uses light scattering, the difference of the scattering lengths between the monomers if one uses neutrons, or the difference of electron densities for X-rays; φ is the total volume fraction of polymer, and χ_{ab} the Flory–Huggins interaction parameter

between polymers A and B. This is an attractive simplification, but it is valid only under certain conditions and we shall discuss this point in more detail later.

The properties of multicomponent polymer mixtures, in the limit of the zero scattering angle, were discussed a long time ago by Stockmayer.[5] Using a thermodynamic method, Stockmayer derived a general formula for scattering in the forward direction, which is consistent with the Flory–Huggins free energy model[6] when applied to the case of ternary mixtures of two polymers and a solvent, or two solvents and a polymer. For several decades,[7–9] this formula served as the basis for the interpretation of light scattering data and the thermodynamic behavior of multicomponent polymer mixtures. Its generalization to finite scattering angles has been worked out relatively recently on the basis of the chain of single contacts model.[3,10] This is an extension of Zimm's single contact approximation[11] which includes interactions between either similar or different chains. The final result provides a mean field evaluation of the scattered intensity for a mixture of two polymers and a solvent. It accommodates for the cases where the contrast with the solvent $\nu_i - \nu_s$, the molecular weights and the interaction parameters of the polymers are, in principle, arbitrary. Within this approximation, it becomes possible to account for the effects of interactions in the whole range of concentration going from the dilute to the semi-dilute regimes and eventually overlapping with the concentrated region. It gives the correct bulk result if one takes properly the limit of $\varphi_s = 0$. Some remarks concerning the extension of the random phase approximation (RPA) using the blob model and renormalization group theory[12–14] will be made in a later section.

In this paper, we focus our attention on mixtures having special optical properties which satisfy the so-called zero average contrast (ZAC) condition. This limit is also known in certain cases as the optical theta condition.[15] One of the first applications of the ZAC method to polymer mixtures was known as the high concentration method. This method was designed to extract single chain properties for a deuterated polymer in a matrix of identical but nondeuterated chains at high concentrations and using the small angle neutron scattering technique.[16–18] In the theoretical part of this paper, it will be shown that only in the ZAC is one allowed to treat the ternary mixture made of two polymers and a solvent as a pseudo-binary mixture with effective parameters as it was mentioned earlier. Several experimental examples are chosen to illustrate various theoretical predictions. For the case of incompressible blends, scattering radiation probes fluctuations in the order parameter which is the composition of the blend. If these fluctuations continue to grow, they may drive the system unstable and induce phase separation.

The kinetics of phase separation in polymer blends is a well documented subject and a good level of understanding on the mechanism of spinodal decomposition has now been reached.[19–21] One cannot pretend that comparable knowledge exists for blends in the presence of a low molecular weight solvent. For these ternary mixtures, at least two order parameters emerge, describing composition and concentration fluctuations. Yet another complication arises due to coupling between these two order parameters. It will be shown that for symmetric mixtures satisfying the ZAC, such coupling disappears and the contribution of the concentration fluctuations to the scattered intensity vanishes. In this case, the treatment of ternary mixtures becomes very simple and the pseudo-binary description is justified. Furthermore, the measurement of the scattering signal is due only to composition fluctuations and gives direct access to important quantities such as the polymer–polymer interaction parameter and the self-diffusion coefficient.

In the first part of this paper, some theoretical predictions concerning static and dynamic properties are made based on mean field approximations and in particular on the random

phase approximation (RPA). In the second part, these theoretical predictions are used to examine a few experimental examples of data obtained by the three major techniques: light, neutrons and X-rays. We have selected only a few examples concerning stable homogeneous mixtures that fulfill the ZAC condition. We consider in particular the systems: (i) ternary mixtures of two homopolymers and a solvent; (ii) diblock copolymers and a solvent; (iii) quaternary mixtures of three homopolymers and a solvent; (iv) polyelectrolytes in aqueous solutions with selective deuterium labelling.

2. THEORETICAL PREDICTIONS

2.1. *Static scattering*

2.1.1. *Scattered intensity and structure factors*

The theory of static light scattering of binary polymer solutions including the inter-chain interactions was put forward by Zimm,[11] who derived the expression for scattered intensity as a function of concentration and scattering angle. This equation was the starting point for the classical Zimm plot analysis which is a major tool for polymer characterization.[22] Zimm plots are performed routinely in major laboratories to characterize newly synthesized polymers and extract basic quantities such as the molecular weight M, the index of polydispersity M_w/M_n, the radius of gyration R_g and the second virial coefficient A_2. In the standard experimental notation, Zimm's equation is given as:

$$KMc/I(q) = 1/P(q) + 2A_2Mc \tag{1}$$

where q, the amplitude of the scattering wave vector, can be expressed in terms of the wavelength λ of the incident radiation, the index of refraction of the medium n and the scattering angle θ by:

$$q = 4\pi n \sin(\theta/2)/\lambda \tag{2}$$

For vertically polarized incident light, the constant K is:

$$K = 4\pi^2 n^2 (\mathrm{d}n/\mathrm{d}c)^2 N_{av}/\lambda^4. \tag{3}$$

If one uses the neutron scattering technique, q has a similar expression as in eqn (2) except that the index of refraction n should be removed, and K replaced by $(v_a - v_s)^2$, the contrast with respect to the solvent squared. In eqn (1), the second virial coefficient A_2 is related to the excluded volume parameter v by:

$$A_2 = vN_{av}/2m_0^2 \tag{4}$$

where m_0 is the molecular weight of the monomer, N_{av} the Avogadro number and $\beta = 1/K_BT$, K_B is the Boltzmann constant and T the absolute temperature. The excluded volume parameter v is related to the effective inter-monomer potential $u(r)$ or to the pair correlation function $g(r) = \mathrm{e}^{-\beta u(r)}$ through the binary cluster integral:

$$v = \int \mathrm{d}^3 r[1 - g(r)] = \int \mathrm{d}^3 r[1 - \mathrm{e}^{\beta u(r)}]. \tag{5}$$

This result can be expressed in terms of the monomer–solvent Flory–Huggins interaction parameter χ_{ms}[6,23] via:

$$v = [v_m^* 2/v_s^*](1/\varphi_s - 2\chi_{ms}) \tag{6}$$

where v_i^* represents the molar volumes of the monomers A, B,⋯, etc. and the solvent S (i.e. i = a, b, ⋯, s).

Let us now go back to Zimm's equation and consider the form factor $P(q)$ which determines the architecture of the polymer. $P(q)$ can be calculated using the definition:

$$N^2P(q) = \sum_{ij} < e^{iq.r_{ij}} > . \tag{7}$$

Here, $N = M/m_0$ is the degree of polymerization, the symbol $< \cdots >$ denotes the average with respect to the equilibrium distribution, and $\mathbf{r}_{ij}$ is the vector distance between monomers i and j along a chain. Assuming a Gaussian distribution for $\mathbf{r}_{ij}$, and approximating discrete sums by integrals yields the Debye function:

$$P(q) = 2(e^{-u} + u - 1)/u^2 \qquad u = q^2R_g^2. \tag{8}$$

For practical purposes, another representation is frequently used for Gaussian chains:[24]

$$P(q) \approx (1 + u/3)^{-1} \tag{9}$$

Besides its convenience, this approximation is quite good in the small q limit where $qR_g < 1$. In the upper q range where $qR_g > 1$, a slightly better representation would be to substitute 1/3 by 1/2 in the above equation. It is sometimes more convenient to use molecular quantities such as (N, v, φ) instead of their experimental counterparts (M, A_2, c). The relationships between these two sets of parameters are:

$$A_2 = vN_{av}/2m_0^2 \qquad M = Nm_0 \qquad c = \varphi\rho \tag{10}$$

where

$$\rho = m_0/v_0$$

is the polymer density.

As an example of equations written in these two representations, one notes that Zimm's equation in the experimental form is:

$$Kc/I(q) = 1/M + 2A_2c + q^2R_g^2/3M \tag{11}$$

and in terms of molecular quantities, it reads:

$$1/S(q) = 1/N\varphi + v/[v_m^{*2}/v_s^*] + q^2R_g^2/(3N\varphi). \tag{12}$$

As we mentioned earlier, this is the basic equation for the characterization of binary polymer mixtures using Zimm plot analysis. Two main assumptions were made to derive this result. The first one is to assume that the solution is dilute and any pair of chains can have only one contact point at a time. This is the single contact approximation. The second approximation is to replace $1 - 2A_2Mc$ by $1/(1 + 2A_2Mc)$ which means that $2A_2Mc$ should remain small as compared to one. This substitution actually means that one includes indirectly higher order interaction terms. This observation probably helps to explain the validity of Zimm's equation at concentrations far beyond the dilute regime.[3,22,25] A characteristic concentration denoted c^* determines roughly the border line between the dilute and the semi-dilute regimes. From the above considerations, an alternative definition of c^* would be:

$$c^* = [2A_2M]^{-1} \tag{13}$$

which can be compared with the classical overlap concentration c^*:[14,25]

$$c^* = M/[4\pi N_{av} R_g^3/3]. \tag{14}$$

Introducing the static swelling factor α_s, where R_{g0} is the radius of gyration of a Gaussian linear chain and σ is the average monomer size, one can write the second virial coefficient A_2 as:

$$A_2 = \text{const.}\alpha_s^3/M^{1/2}. \tag{15}$$

The constant is equal to $\pi N_{av}/[9\sqrt{6}m_0^3]$ and

$$\alpha_s^2 = [R_g^2/R_{g0}^2] \qquad R_{g0}^2 = N\sigma^2/6. \tag{16}$$

In the vicinity of theta temperature, α_s is close to one and eqn (15) shows that A_2 goes to zero as $M^{-1/2}$. If the excluded volume interaction is strong, using $R_g \sim N^{3/5}$, one finds that

$$\alpha_s \sim M^{0.1}.$$

The second virial coefficient A_2 has a much weaker dependence upon M and is consistent with the universal scaling law obtained by de Gennes:[14]

$$A_2 \sim M^{-0.2}. \tag{17}$$

However, this result is slightly different from the one obtained by neutron scattering of polystyrene in a good solvent:[26]

$$A_2 = 1.04 \times 10^{-2} M^{-0.254} \tag{18}$$

and for polydimethylsiloxane:[27]

$$A_2 = 0.71 \times 10^{-2} M^{-0.25}. \tag{19}$$

It was pointed out earlier that the theory of static scattering from multicomponent polymer mixtures was first developed by Stockmayer[5] using a thermodynamic method. The formula derived by Stockmayer describing the scattering intensity in the forward direction ($q = 0$) turned out to be consistent with the Flory–Huggins free energy model and de Gennes RPA in the case of homopolymer blends. These mean field theories lead to the same result which can be written as:

$$I(q=0) = (\nu_a - \nu_b)^2 S(q=0) \tag{20}$$

where the structure factor at $q = 0$ is given by:

$$1/S(q=0) = 1/[N_a\varphi_a] + 1/[N_b\varphi_b] - 2\chi_{ab}. \tag{21}$$

χ_{ab} is the Flory–Huggins interaction parameter. If component B has a low molecular weight and can be considered as a solvent, $N_b = 1$ and the above formula reduces to Zimm's equation at $q = 0$. On the other hand, the extension of eqn (21) to finite q is straightforward and can be implemented simply by including the form factors $P_a(q)$ and $P_b(q)$:

$$1/S(q) = 1/[N_a\varphi_a P_a(q)] + 1/[N_b\varphi_b P_b(q)] - 2\chi_{ab}. \tag{22}$$

For a multicomponent mixture, the scattering intensity one would obtain in a generalization of Stockmayer's theory to finite q is:[3,28–30]

$$\mathbf{I(q)} = \boldsymbol{\upsilon}^{\mathrm{T}}\mathbf{S(q)}\boldsymbol{\upsilon} \tag{23}$$

where $\boldsymbol{v}$ is a column vector whose elements are the increments of refractive indices, the contrast factors or the electron densities, and $\boldsymbol{v}^T$ its transpose. One can write the structure matrix $\mathbf{S(q)}$ for a multicomponent mixture within the RPA as:[3,11,14]

$$\mathbf{S(q)}^{-1} = \mathbf{S}_0(\mathbf{q})^{-1} + \mathbf{v}. \tag{24}$$

If all the constituants of the mixture are homopolymers, the elements of $\mathbf{S}_0(\mathbf{q})$ are simply:

$$S_{0i}(q) = N_i \varphi_i P_i(q) \qquad i = a, b, c \text{ etc.} \tag{25}$$

The excluded volume parameters v_{ij} can also be generalized from eqn (6):

$$v_{ii} = [v_{im}^{*2}/v_s^*](1/\varphi_s - 2\chi_{is})$$

$$v_{ij} = [v_i^* v_j^*/v_s^*](1/\varphi_s - \chi_{is} - \chi_{js} + \chi_{ij}) \text{ if } i \neq j. \tag{26}$$

This is a general formalism which is applied to various systems in the following sections.

2.1.2. *Ternary mixtures of homopolymer A/homopolymer B/solvent*

In the case of a ternary mixture made of two homopolymers A and B and a solvent, eqns (23)–(26) yield:

$$I(q) = (v_a - v_s)^2(1/S_{0a} + 1/\varphi_s - 2\chi_{as}) + (v_b - v_s)^2(1/S_{0b} + 1/\varphi_s - 2\chi_{bs})$$
$$- 2(v_a - v_s)(v_b - v_s)(1/\varphi_s - \chi_{as} - \chi_{bs} + \chi_{ab})\}/$$
$$\{[1/S_{0a} + 1/\varphi_s - 2\chi_{as}][1/S_{0b}(q) + 1/\varphi_s - 2\chi_{bs}] - (1/\varphi_s - \chi_{as} - \chi_{bs} + \chi_{ab})^2\}. \tag{27}$$

This is a mean field result which is nevertheless useful for practical purposes. For example, the limit of thermodynamic stability is defined by $\det.\mathbf{S}^{-1} > 0$ and the spinodal equation is given by $\det.\mathbf{S}^{-1} = 0$. This equation provides a relationship between the volume fractions, the degrees of polymerization and the interaction parameters:

$$(1/N_a\varphi_a + 1/\varphi_s - 2\chi_{as})(1/N_b\varphi_b + 1/\varphi_s - 2\chi_{bs}) - (1/\varphi_s - \chi_{as} - \chi_{bs} - \chi_{ab})^2 = 0. \tag{28}$$

Regarding the "optical conditions", one can consider different cases depending upon the values of v_a, v_b and v_s. Although our primary interest in this chapter is to examine systems fulfilling the ZAC, it is nonetheless useful to consider briefly the case where B is isorefractive with the solvent (i.e. $v_b = v_s$). This case is commonly considered in the literature and it would be interesting to compare these predictions to those obtained under the ZAC.

2.1.2.1. *Polymer B isorefractive with the solvent* – Let us consider an example in the following way. Starting from the binary solution of polymer A and solvent such as polystyrene (PS) and toluene at a given concentration, let us add to this mixture the second polymer B which is isorefractive with the solvent, say poly (methyl-methacrylate) or PMMA. A question one could ask in this hypothetical system is to what extent PMMA modifies the scattering properties of PS. Although the radiation probes directly the

fluctuations in the concentration of A, the scattering signal should be nevertheless strongly influenced by the presence of B in the solution. The scattered intensity $I(q)$ is proportional to the partial structure factor $S_{aa}(q)$ which can be easily obtained from eqn (27):

$$1/S_{aa}(q) = 1/N_a\varphi_a P_a(q) + v_{aa} - v_{ab}^2\varphi_b N_b P_b/(1 + v_{bb}N_b\varphi_b P_b(q)) \tag{29}$$

In the experimental notation, the scattered intensity $I(q)$ is proportional to $S_{aa}(q)$ and is:

$$K_a M_a c_a/I(q) = 1/P_a(q) + 2A_{2a}M_a c_a - 4A_{2ab}^2 M_a M_b c_a c_b P_b(q)/(1 + 2A_{2b}M_b c_b P_b(q)). \tag{30}$$

Clearly, the third term in the right hand side (RHS) of this equation describes the effect of the invisible polymer B. Using the approximate form of $P(q)$ in eqn (9), one can write this result in terms of an apparent second virial coefficient $A_{2a,ap}$ and an apparent radius of gyration $R_{ga,ap}$:

$$K_a M_a c_a/I_a(q) = 1 + 2A_{2a,ap}M_a c_a + q^2 R_{ga,ap}^{2/3}. \tag{31}$$

$A_{2a,ap}$ and $R_{ga,ap}$ are directly accessible from the Zimm plot analysis. Introducing the overlap concentration $c_b^* = (2A_{2b}M_b)^{-1}$, one can express these quantities in terms of the interactions between species in the mixture. For example, the reduced apparent virial coefficient is found as:

$$A_{2ap}/A_{2a} = 1 - 2A_{2ab}^2 M_b(c_b/c_b^*)/[A_{2a}A_{2b}(1 + c_b/c_b^*)]. \tag{32}$$

This quantity may be reduced substantially if c_b is large as compared to c_b^*. The asymptotic limit where $c_b >> c_b^*$ is

$$A_{2a,ap}/A_{2a} = 1 - A_{2ab}^2/A_{2a}A_{2b}. \tag{33}$$

The matrix (PMMA + toluene) behaves as a theta solvent if $A_{2ab} = \sqrt{A_{2a}A_{2b}}$ and becomes a bad solvent if $A_{2ab} > \sqrt{A_{2a}A_{2b}}$. In the dilute range (i.e. $c_b < c^*_b$), the reduction of the apparent quality of solvent is proportional to c_b/c_b^* as shown by:

$$A_{2a,ap}/A_{2a} = 1 - [A_{2ab}^2/(A_{2a}A_{2b})](c_b/c_b^*). \tag{34}$$

A similar analysis can be made for the apparent radius of gyration one would obtain from the Zimm plot.

The problem is entirely different if chains A and B are linked together to form a diblock copolymer A–B. Unlike homopolymers, the bare structure matrix has a non-zero off-diagonal element:

$$S_{0ab}(q) = S_{0ba}(q) = x(1-x)N\varphi P_{ab}(q) \tag{35}$$

which describes the intra-chain correlations between species A and B. The form factor $P_{ab}(q)$ can be calculated directly or simply deduced from the geometrical relationship:[3]

$$P(q) = x^2 P_a(q) + (1-x)^2 P_b(q) + 2x(1-x)P_{ab}(q) \tag{36}$$

where $P(q)$ designates the total chain form factor and x the composition of monomers A within the chain (i.e. $x = N_a/N$, $N = N_a + N_b$). For Gaussian chains, $P_a(q)$, $P_b(q)$ can be described by the Debye function using $u_a = q^2\sigma_a^2 N_a/6$ and $u_b = q^2\sigma_b^2 N_b/6$, respectively. For a Gaussian chain, a direct calculation of $P_{ab}(q)$ gives:

$$P_{ab}(q) = (1 - e^{-u_a})(1 - e^{-u_b})/u_a u_b. \tag{37}$$

Following the treatment in the homopolymer case, it would be interesting to consider briefly the case where $v_b = v_s$ and B is isorefractive with the solvent. The relevent structure

factor is $S_{aa}(q)$:

$$S_{aa}(q) = [S_{0a}(q) + v_{bb}\Delta S_0(q)]/$$

$$[1 + v_{aa}S_{0a}(q) + v_{bb}S_{0b}(q) + 2v_{ab}S_{0ab}(q) + (v_{aa}v_{bb} - v_{ab}^2)\Delta S_0(q)] \quad (38)$$

with

$$S_{0a}(q) = x^2 N\varphi P_a(q) \quad (39a)$$

$$S_{0b}(q) = (1-x)^2 N\varphi P_b(q) \quad (39b)$$

$$S_{0ab}(q) = x(1-x)N\varphi P_{ab}(q) \quad (40a)$$

$$\Delta S_0(q) = S_{0a}(q)S_{0b}(q) - S_{0ab}(q)^2. \quad (40b)$$

In the reciprocal form, one has perhaps a more appealing result:

$$1/S_{aa}(q) = 1/S_{0a}(q) + v_{aa}$$
$$- [v_{ab}^2 S_{0a}(q)\Delta S_0(q) - v_{bb}S_{0ab}^2(q) - 2v_{ab}S_{0a}(q)S_{0ab}(q)]/$$
$$[S_{0a}(q)(S_{0a}(q) + v_{bb}\Delta S_0(q))]. \quad (41)$$

Letting $S_{0ab}(q) = 0$, one recovers the result for the homopolymer mixture. Furthermore, in the forward direction, noting that $\Delta S_0(q = 0) = 0$, one obtains:

$$x^2 N\varphi/S_{aa}(0) = 1 + v_{cop,ap}x^2 N\varphi \quad (42)$$

where the apparent excluded volume parameter for the copolymer $v_{cop,ap}$ is:

$$v_{cop,ap} = [x^2 v_{aa} + (1-x)^2 v_{bb} + 2x(1-x)v_{ab}]/x^2 \quad (43)$$

which is similar to the case of a single homopolymer in a solvent with an excluded volume parameter which takes into account the connectivity of chains and the interaction of unalike monomers v_{ab}. We shall come back to the copolymer problem shortly. We conclude this section by noting that for the corresponding homopolymers, the result is:

$$x^2 N\varphi/S_{aa}(0) = 1 + v_{hom,ap}x^2 N\varphi \quad (44)$$

$$v_{hom,ap} = v_{aa}\{1 - v_{ab}^2\varphi_b N_b/[v_{aa}(1 + v_{bb}\varphi_b N_b)]\}. \quad (45)$$

2.1.2.2. *Homopolymers A and B in a solvent under the ZAC* – One of the pionnering applications of the ZAC to ternary mixtures comprised of two polymers and a solvent using light scattering was due to Fukuda *et al.*[15] These authors used a different terminology referring to this condition as the optical theta condition. In their treatment, Fukuda *et al.* considered only the forward scattering at $q = 0$ and the dilute limit assuming that φ_a and φ_b are small compared to φ_a^* and φ_b^*. They obtained the forward scattering intensity in the form:

$$I(q=0) = (v_a - v_s)^2\varphi_a N_a + (v_b - v_s)^2\varphi_b N_b - 2\chi_{ab}(v_a - v_s)(v_b - v_s)\varphi_a\varphi_b N_a N_b$$
$$- 2[(v_a - v_s)v_{aa}\varphi_a N_b + (v_b - v_s)v_{bb}\varphi_b N_b][(v_a - v_s)\varphi_a N_a + (v_b - v_s)\varphi_b N_b] \quad (46)$$

and their motivation was to propose a new method for the measurement of the interaction parameter χ_{ab} which would be independent of the polymer–solvent interaction parameters χ_{as} and χ_{bs}. In the limit which they referred to as the ''optical theta'', one has:

$$(v_a - v_s)\varphi_a N_a + (v_b - v_s)\varphi_b N_b = 0. \tag{47}$$

Substituting this into eqn (46) yields:

$$S(q=0)/\varphi N = (v_a - v_s)^2 x^2 + (v_b - v_s)^2 (1-x)^2 - 2\chi_{ab}(v_a - v_s)(v_b - v_s)x^2(1-x)^2 \varphi N \tag{48}$$

This result suggests that the variation of $S(q = 0)/\varphi$ vs φ gives a linear decrease with a slope that is proportional to χ_{ab}, regardless of the polymer–solvent interaction parameters χ_{as} and χ_{bs}. This procedure was used by Fukuda *et al.* to measure χ_{ab} for mixtures of PS/PMMA in bromobenzene with different molecular weights using static light scattering. The generalization of this procedure to finite q and finite concentration can be achieved only for symmetrical mixtures assuming equal degrees of polymerization, form factors and interactions with the solvent in addition to a 50/50 composition:

$$N_a = N_b = N \qquad P_a(q) = P_b(q) = P(q) \qquad \chi_{as} = \chi_{bs} = \chi_0 \; x = 1/2. \tag{49}$$

These conditions imply that the bare structure factors are equal

$$S_{0a} = S_{0b} = S_0 = N\varphi P(q)/2. \tag{50}$$

The excluded volume parameters of A and B are the same

$$v_{aa} = v_{bb} = v \tag{51a}$$

The relationship between χ_{ab} and the excluded volume parameters is:

$$\chi_{ab} = v_{ab} - (v_{aa} + v_{bb})/2. \tag{51b}$$

Combining these equations leads to:

$$S(q)/\varphi^2 = [(v_a - v_s)\varphi_a + (v_b - v_s)\varphi_b]^2 N\varphi P(q)/[1 + vN\varphi P(q)] + \{[(v_a - v_s)\varphi_a - (v_b - v_s)\varphi_b]/\varphi\}^2 N\varphi P(q)/[1 - 2\chi_{ab}x(1-x)N\varphi P(q)]. \tag{52}$$

If the average contrast is zero, one has:

$$(v_a - v_s)\varphi_a + (v_b - v_s)\varphi_b = 0, \tag{53}$$

and the structure factor $S(q)$ becomes

$$S(q) = [(v_a - v_b)/2]^2 N\varphi P(q)/[1 - 2\chi_{ab}\varphi x(1-x)NP(q)]. \tag{54}$$

This result is similar to the signal one would obtain from a pure blend with an apparent contrast factor $(v_a - v_b)_{ap} = \varphi(v_a - v_b)$ and an apparent interaction parameter $\chi_{ap} = \varphi\chi_{ab}$. Both quantities are reduced by the presence of solvent. The decrease in the interaction parameter means that the blend shows an enhanced compatibility in the presence of solvent.

Comparison of eqn (47) and eqn (53) shows that the ZAC, unlike the optical theta condition, does not involve the degrees of polymerization. However, if the polymers have the same

degree of polymerization, the ZAC and the optical theta conditions become identical. It is worth noting that at $q = 0$, eqn (54) gives the same result as Fukuda *et al.* although the latter was derived only in the limit of small concentrations. For symmetrical mixtures, this constraint on the concentration regime does not exist and the same procedure can be used to measure the interaction parameter. This will be demonstrated with a few practical examples which we shall consider in the experimental section.

2.1.3. *Quaternary mixtures under the ZAC*

Recently, Strazielle *et al.*[31–33] reported static and dynamic light scattering data from polymer mixtures of PS/PDMS/PMMA/toluene. The increment of refractive index of PMMA in toluene is approximately zero

$$\partial n/\partial c_{\mathrm{PMMA}} \approx 0$$

meaning that this polymer is not visible for the probing radiation. On the other hand, PS and PDMS have increments of refractive indices approximately equal in magnitude with opposite signs:

$$\partial n/\partial c_{PS} \approx \partial n/\partial c_{\mathrm{PDMS}}.$$

The ZAC is satisfied if the composition $x = \varphi_{\mathrm{PS}}/(\varphi_{\mathrm{PS}} + \varphi_{\mathrm{PDMS}})$ is 1/2. In this case, the intensity one measures is directly proportional to the structure factor $S(q)$:

$$S(q)/\varphi^2 = S_{\mathrm{aa}}(q)/\varphi_{\mathrm{a}}^2 + S_{\mathrm{bb}}(q)/\varphi_{\mathrm{b}}^2 - 2S_{\mathrm{ab}}(q)/\varphi_{\mathrm{a}}\varphi_{\mathrm{b}} \tag{55}$$

where $S_{ij}(q)$ $(i, j = a, b)$, are obtained from the inversion of the matrix in eqn (24). Since we are interested in symmetrical mixtures, we have $\chi_{\mathrm{cs}} = \chi_{\mathrm{as}}$ in addition to eqn (49), which means that PMMA has the same interaction with toluene as PS and PDMS. For convenience, the subscripts a and b will refer to PS and PDMS, respectively, whereas the quantities referring to PMMA will be primed. Hence, the matrix equation becomes very simple:

$$S^{-1}(q) = \begin{bmatrix} S_0(q)^{-1} + v & v + \chi_{\mathrm{ab}} & v \\ v + \chi_{\mathrm{ab}} & S_0(q)^{-1} + v & v + \chi_{\mathrm{ab}} \\ v & v + \chi_{\mathrm{ab}} & S'_0(q)^{-1} + v \end{bmatrix}. \tag{56}$$

The bare structure factors $S_0(q)$ and $S'_0(q)$ are:

$$S_0 = (q) = N\varphi P(q)/4 \qquad S'_0(q) = \varphi' N' P'(q) \tag{57}$$

and S_{ij} can be obtained from the inversion of the above matrix. Substituting the results into eqn (55) yields:

$$\varphi/S(q) = [4\varphi/S_0(q)][1 + 2vS_0(q) + vS_0'(q) - \chi_{\mathrm{ab}}(\chi_{\mathrm{ab}} + 2v)S_0(q)(S_0(q) + S_0'(q))]/$$
$$[2(1 + 2vS_0(q) + vS_0'(q)) - \chi_{\mathrm{ab}}(\chi_{\mathrm{ab}} + 2v)S_0(q)S_0'(q) + 2\chi_{\mathrm{ab}}S_0(q)]. \tag{58}$$

In obtaining this result, we have allowed the properties of PMMA to be different from those of PS and PDMS in order to cover a more general case. Introducing an apparent interaction parameter and a correlation length ξ, one can put the result in the form:

$$\varphi/S(q) = \varphi/S(q = 0)[1 + q^2\xi^2]. \tag{59}$$

The structure factor in the forward direction $S(q = 0)$ is such that:

$$\varphi/S(q=0) = 4/N - 2\varphi\chi_{ap}. \tag{60}$$

The apparent interaction parameter is:

$$\chi_{ap} = \chi_{ab}[1 + (\chi_{ab}/2 + v)(N\varphi + N'\varphi')]/[1 + (\chi_{ab}/2 + v)(1 - \chi_{ab}N'\varphi'/2)N\varphi + vN'\varphi'] \tag{61}$$

and the correlation length ξ is given by:

$$\xi^2 = [R_g^2/3][1 - 3L^2\chi_{ab}/\chi_0 R_g^2]/[1 - \chi_{ap}/\chi_0] \tag{62}$$

where χ_0 is the critical parameter in the mean field limit:

$$\chi_0 = 2/N\varphi$$

and the length L is defined by:

$$L^2 = [AB - CD]/C^2$$

with

$$A = 1 + (v + \chi_{ab}/2)[N\varphi + N'\varphi']$$

$$B = (v + \chi_{ab}/2)N\varphi R_g^2/3 + vN'\varphi' R_g'^2/3 - (v + \chi_{ab}/2)\chi_{ab}N\varphi N'\varphi'(R_g^2 + R_g'^2)/6$$

$$C = 1 + (v + \chi_{ab}/2)N\varphi + [v - \chi_{ab}(v + \chi_{ab}/2)N\varphi/2]N'\varphi'$$

$$D = (v + \chi_{ab}/2)[N\varphi R_g^2 + N'\varphi' R_g'^2]/3$$

One observes that the scattered intensity grows more rapidly when the concentration of PMMA increases. However, this increase in scattering is more important as q tends to zero indicating that the fluctuations of long wavelengths have the dominant contribution to the scattering. The critical concentration φ_K, at which phase separation via spinodal decomposition occurs, is lowered by an amount proportional to φ'. The critical concentration can be evaluated from the spinodal equation which is the condition under which the scattered intensity diverges or $\det.S^{-1}(q = 0) = 0$:

$$N(\chi/2 + v)\varphi_K^2 + 2[(\chi/2 + v)N'\varphi' - v/\chi]\varphi_K - 2(1 + vN'\varphi')/N\chi = 0 \tag{63}$$

The resolution of this equation yields:

$$\varphi_K = \varphi_{0K}\left\{v/(\chi + 2v) + [(\chi + v)/(\chi + 2v)^2 + (\chi N'\varphi'/2)^2]^{1/2}\right\}$$

$$-N'\varphi'/N \approx \varphi_{0K} - N'\varphi'/N \tag{64}$$

where φ_{0K} is the critical concentration in the absence of PMMA.

$$\varphi_{0K} = 2/N\chi. \tag{65}$$

Equation (64) indicates that φ_K shifts towards smaller values when the amount of PMMA is increased. An estimate of this shift is given. In the next section, we discuss the properties of diblock copolymers in solution.

2.1.4. *Solutions of diblock copolymers AB under the ZAC*

An analysis similar to the one given above for homopolymer blends can be applied to diblock copolymers AB in a solvent under the ZAC. First note that at $q = 0$, the diblock appears as a single homopolymer, its internal structure cannot be resolved, and the procedure used by Fukuda *et al.* in the case of homopolymers to measure the χ-parameter is not applicable here. One needs to consider the scattering at a finite q in order to explore the internal structure of the copolymer and to have access to the interaction parameter for microphase separation. For simplicity, we limit ourselves to the case of a symmetric copolymer in which the two blocks A and B have similar dimensions. In this case, the scattered intensity takes a simple form making a direct evaluation of the χ-parameter feasible. This can be shown by first considering the general form of the scattered intensity for a diblock AB in solution:

$$I(q) = \{(v_a - v_s)^2[S_{0a}(q)/\Delta S_0(q) + v_{bb}] + (v_b - v_s)^2[S_{0b}(q)/\Delta S_0(q) + v_{aa}] + 2(v_a - v_s)(v_b - v_s)[S_{0ab}/\Delta S_0(q) - v_{ab}]\}/\{[S_{0a}(q)/\Delta S_0(q) + v_{bb}] \times [S_{0b}(q)/\Delta S_0(q) + v_{aa}] - [S_{0ab}/\Delta S_0(q) - v_{ab}]^2\}. \quad (66)$$

This result is to be compared with eqn (46) for the homopolymer counterpart. The bare structure factors for this system have already been defined in eqns (39) and (40). The forward scattering intensity $I(q = 0)$ has been given in eqn (2) and eqn (43) in the case where block B is isorefractive with the solvent. Here, the focus is put onto the diblock copolymer under the ZAC. For a symmetrical diblock under this condition, one has a direct access to the χ-parameter from the measurement of $I(q)$:

$$I(q) = [(v_a + v_b)/2 - v_s]^2 N\varphi P(q)/[1 + (v + \chi/2)\varphi N P(q)] + [(v_a - v_b)/2]^2 N\varphi[P_{1/2}(q) - P(q)]/\{1 - \chi_{ab} N\varphi[P_{1/2}(q) - P(q)]/2\}. \quad (67)$$

In the ZAC, $v_a + v_b = 2v_s$ and $I(q)$ becomes:

$$(v_a - v_b)^2/I(q) = 4/[N\varphi(P_{1/2}(q) - P(q))] - 2\chi_{ab}. \quad (68)$$

The plot of $I(q)$ versus q^2 shows a maximum at the wave vector $q^* \sim 1/R_g$ and the critical parameter $\chi = \chi^*_{ab}$ for which $I^{-1}(q = q_m) = 0$ is obtained from:

$$N\varphi\chi^*_{ab} = 2/[P_{1/2}(q^*) - P(q^*)] \approx 10. \quad (69)$$

Hashimoto and co-workers[34] performed a comparative study of the scattering from block copolymers in solution using both eqn (67) and the pseudo-binary treatment based on Leibler's formula with apparent parameters. They came to the conclusion that under the ZAC, both models predict similar results. Hashimoto and co-workers[34,35] also performed X-ray measurements under this condition and found a good agreement with eqn (67). This point will be discussed further in the Section 3 of this review.

2.1.5. *Critical fluctuations and the scaling behavior under the ZAC*

In this section, we discuss the scaling behavior of static and dynamic scattering properties of ternary mixtures of polymer A/polymer B/solvent in the vicinity of the critical temperature.

For reasons that will become clear shortly after, the scattered intensity $I(q)$ is written in terms of a new structure matrix $\check{\mathbf{S}}(q)$:[3,29,30,36]

$$I(q) = v^{\mathrm{T}}\check{\mathbf{S}}(q)v. \tag{70}$$

$\check{\mathbf{S}}(q)$ is obtained from $\mathbf{S}(q)$ by the transformation Λ

$$\check{\mathbf{S}}(q) = \Lambda^{\mathrm{T}}\mathbf{S}(q)\Lambda \tag{71}$$

with

$$\Lambda = \begin{bmatrix} 1 & 1-x \\ 1 & -x \end{bmatrix}. \tag{72}$$

Combining eqns (70)–(72) yields:

$$\check{\mathbf{S}}(q) = \begin{bmatrix} S_{\mathrm{cc}} & S_{\mathrm{cx}} \\ S_{\mathrm{xc}} & S_{\mathrm{xx}} \end{bmatrix} \tag{73}$$

where S_{cc} and S_{xx} are the structure factors for concentration and composition fluctuations, respectively, whereas $S_{\mathrm{xc}} = S_{\mathrm{cx}}$ is the partial structure factor for the coupling between them. One obtains these quantities as combinations of the S_{ij}s:

$$S_{\mathrm{cc}}(q) = S_{\mathrm{aa}}(q) + S_{\mathrm{bb}} + 2S_{\mathrm{ab}}(q), \tag{74}$$

$$S_{\mathrm{xx}}(q) = (1-x)^2 S_{\mathrm{aa}}(q) + x^2 S_{\mathrm{bb}}(q) - 2x(1-x)S_{\mathrm{ab}}(q) \tag{75}$$

$$S_{\mathrm{xc}}(q) = S_{\mathrm{cx}}(q) = (1-x)[S_{\mathrm{aa}}(q) + S_{\mathrm{ba}}(q)] - x[S_{\mathrm{bb}}(q) + S_{\mathrm{ab}}(q)]. \tag{76}$$

Substituting into eqn (70) yields:

$$\begin{aligned} I(q) = {} & [x(v_{\mathrm{a}} - v_{\mathrm{s}}) + (1-x)(v_{\mathrm{b}} - v_{\mathrm{s}})]^2 S_{\mathrm{cc}}(q) + [v_{\mathrm{a}} - v_{\mathrm{b}}]^2 S_{\mathrm{xx}}(a) \\ & + 2[x(v_{\mathrm{a}} - v_{\mathrm{s}}) + (1-x)(v_{\mathrm{b}} - v_{\mathrm{s}})](v_{\mathrm{a}} - v_{\mathrm{b}})S_{\mathrm{xc}}(x). \end{aligned} \tag{77}$$

For a symmetrical system, one has $S_{\mathrm{aa}}(q) = S_{\mathrm{bb}}(q)$ and $S_{ab}(q) = S_{ba}(q) = 0$. One observes that the coupling between concentration and composition fluctuations vanishes when $x = 1/2$ and $S_{\mathrm{cx}} = S_{\mathrm{xc}} = 0$. The matrix $\check{\mathbf{S}}(q)$ becomes:

$$\check{\mathbf{S}}(q) = \begin{bmatrix} S_{\mathrm{aa}}(q) + S_{\mathrm{bb}}(q) + 2S_{\mathrm{ab}}(q) & 0 \\ 0 & [S_{\mathrm{aa}}(q) + S_{\mathrm{bb}}(q) - 2S_{\mathrm{ab}}(q)]/4 \end{bmatrix}. \tag{78}$$

In the ZAC, the first and last terms in the right hand side of eqn (77) vanish and the scattered intensity is directly proportional to $S_{\mathrm{xx}}(q)$. Moreover, regarding the fact that we are interested in long range fluctuations with long wavelengths, one can use eqn (9) and write:

$$S_{\mathrm{xx}}(q)^{-1} = S_{\mathrm{xx}}(q=0)^{-1}[+q^2\xi^2]. \tag{79}$$

In the limit of forward scattering:

$$S_{\mathrm{xx}}(q=0)^{-1} = 2(\chi_0 - \chi_{\mathrm{ab}}). \tag{80}$$

ξ keeps the same value as in eqn (62) in which we let φ', the concentration of the third

polymer PMMA, be zero, or $L = 0$:

$$\xi^2 = R_g^2/[3(1 - \chi_{ab}/\chi_0)]. \tag{81}$$

Instead of using the χ-parameters, these results can be written in terms of the temperatures T and T_0 by using the usual temperature laws:

$$\chi_{ab} = \alpha/T + \beta, \quad \chi_0 = \alpha/T_0 + \beta, \tag{82}$$

where α and β are constants independent of T representing the enthalpic and entropic contributions to the interaction parameters, respectively. Introducing ε, one can express the results in terms of the scaling laws:

$$S_{xx}(q=0)^{-1} = 2\alpha/T_0\varepsilon^{-\gamma}, \tag{83}$$

$$\xi = R_g[T_0\chi_0/3\alpha]^{1/2}\varepsilon^{-\nu}. \tag{84}$$

Showing the divergence of $S_{xx}(q = 0)$ and ξ near the critical temperature with power laws governed by the exponents γ and ν. In the present mean field description, the critical exponents are $\gamma = 1$ and $\nu = 0.5$. In the Ising model, the divergence occurs but with differents exponents which are of the Ising type $\gamma = 1.23$ and $\nu = 0.63$.

The above equations are derived within the mean field model and their validity becomes questionable in the vicinity of the critical region where strong fluctuations take place. Nevertheless, the mean field results are useful in providing a first guess of what could be happening in the region of small ε by extrapolating the behavior observed in the mean field region to the region where the scattered intensity diverges. The data obtained in the case of ternary mixtures indicate that the mean field approximation provides a good description for the scattering behavior far from T_0. As this temperature is approached and ε becomes small, important deviations from the mean field results are observed and the extrapolation procedure becomes questionable. For example, the critical temperature at which $S_{xx}(q = 0)^{-1} = 0$ is found to be different from T_0 obtained by extrapolating the mean field data. We shall come back to these questions in the second part of this paper where experimental examples are discussed.

2.1.6. *Some remarks on renormalization group theory*

Using renormalization group theory arguments, one can represent the interacting polymers as new chains made of renormalized units or blobs. Each polymer is a chain of blobs and different species interact via an effective χ-parameter. The scaling functions are obtained from the perturbation theory in terms of this interaction parameter and in the first order, the results are referred to as the zero loop RPA calculations. The results show that the effective χ-parameter is a function of various quantities such as the degree of polymerization and the concentration. They indicate a better fit with the data of Fukuda *et al.* for PS/PMMA/bromobenzene than the standard RPA.[15,37] However, this approximation is not sufficient in describing other effects and the next order approximation, or the one order loop, is required. For example, computer simulations have revealed that the size of minority chains in a blend are contracted in comparison with their size in the theta state.[38] This behavior cannot be predicted by the standard RPA or by its one-loop renormalized version.

To understand some of these points, we consider only a few steps in the renormalization group theory approach. In the lattice model, assuming that monomers A and B and a solvent molecule occupy equal volume, one can write the free energy per lattice site:[6]

$$F_0/k_BT = (\varphi_a/N_a)\ln\varphi_a + (\varphi_b/N_b)\ln\varphi_b + \varphi_s\ln\varphi_s + \chi_{as}\varphi_a\varphi_s + \chi_{bs}\varphi_b\varphi_s + \chi_{ab}\varphi_a\varphi_b. \quad (85)$$

In a dilute solution where φ_s is close to one, using the excluded volume parameters

$$v_{aa} \approx 1 - 2\chi_{as},\ v_{bb} \approx 1 - 2\chi_{bs} \text{ and } v_{ab} \approx 1 - \chi_{as} - \chi_{bs} + \chi_{ab},$$

one can put the free energy in the form:

$$F_0/k_BT = (\varphi_a/N_a)\ln\varphi_a + (\varphi_b/N_b)\ln\varphi_b + \{v_{aa}\varphi_a^2 + v_{bb}\varphi_b^2 + 2v_{ab}\varphi_a\varphi_b\}/2 + \ldots. \quad (86)$$

One can write another expression for the free energy by defining a new lattice with a characteristic size ξ. The renormalized free energy in this coarse-grained system is:

$$F_0/k_BT = (a/\xi)^3 F_{blob}/k_BT + v_{aa}(a/\xi)^3/2 + \ldots. \quad (87)$$

This leads to a new description of the system which, following Brosetta *et al.*,[39] is a mixture in which the chains can be visualized as successions of uncorrelated subunits or blobs having a molecular weight M_{blob} and occupying a volume $\xi^3 = M_{blob}/c$. The mixture behaves as a pseudo-binary blend of A and B Gaussian chains. Calling N_a the number of blobs per chain A, ϕ their composition, N_b and $1 - \phi$ the corresponding values for the B chains, denoting the renormalized interaction parameter χ_{blob}, Brosetta *et al.* obtained the free energy in the coarse-grained system as:

$$F_{blob}/kT = (\phi/N_a)\ln\phi + [(1-\phi)/N_b]\ln(1-\phi) + \chi_{blob}\phi(1-\phi) \quad (88)$$

which is the usual Flory–Huggins free energy expressed in terms of the interaction parameter:

$$\chi_{blob} \approx v_{ab} - (v_{aa} + v_{bb})/2. \quad (89)$$

In the dilute range, the blob size ξ is comparable to the mean radius of gyration R_g. In a semi-dilute solution, ξ is simply the correlation length for monomer concentration fluctuations, and in the concentrated regime, it is comparable to the segment length σ. Broseta *et al.* used these results to discuss the demixing transition of incompatible blends dissolved in a common good solvent. They found that near the demixing transition, composition fluctuations become dominant and are characterized by critical exponents of the Ising type. They observed that the scaling properties of polymers are slightly different from those of small molecules for where the scaling is described by Ising exponents with the Ficher renormalization corrections. They examined the scaling behavior of several quantities such as the interpenetration function:

$$\Delta\psi = [\psi_{AB} - (\psi_{AA} + \psi_{BB})/2] \quad (90)$$

and the second virial coefficient A_{2ab} or the interaction parameter χ_{blob}:

$$\chi_{blob} \approx \Delta A_2 = A_{2ab} - (A_{2aa} + A_{2bb})/2. \quad (91)$$

The scaling with the molecular weight M was found for the interpenetration function as

$$\Delta\psi \sim M^{-0.22} \quad (92a)$$

and for the interaction parameter as:

$$\chi_{\text{blob}} \sim M^{-0.45} \tag{92b}$$

These exponents were calculated by a direct renormalization method to the second order in the parameter $4 - d$ (d being the dimensionality of space, i.e. $d = 3$). The exponent of χ_{blob} is $\delta = 2 + \alpha - 3\nu$ and is equal to 0.45 for $\nu = 0.588$ and $\alpha = 0.22$. Furthermore, χ_{blob} is found to scale with the concentration as:

$$\chi_{\text{blob}} \sim c^{0.3} \tag{93}$$

where the exponent 0.3 is obtained from the scaling law $\alpha/(3\nu - 1)$ using $\alpha = 0.22$ and $\nu = 0.588$. Brosetta *et al.* observed that for weakly interacting polymers, the demixing occurs deep inside the semi-dilute regime where strong overlapping takes place. The critical concentration at which the mixture undergoes phase separation c_K was also examined and its scaling with the molecular weight was derived using the same method. The result is:

$$c_K \sim M^{-0.455}. \tag{94}$$

In some of the experimental examples to be discussed in the second part, we will show how these results compare with the data. Other investigations based upon similar renormalization arguments have also been reported in the literature, in particular those by Onuki and Hashimoto[40] and Schafer and Kappeler.[41]

2.2. *Dynamic scattering properties*

2.2.1. *Equations of motion*

The dynamics of polymer blends have been the subject of intensive investigations in the last few decades.[3,14,24,28,29,42] The main motivation of the early investigations was to understand the mechanism of single chain diffusion and to see whether the reptation model proposed by de Gennes[14] was able to explain the experimental data and the scaling behavior of dynamic properties such as the diffusion coefficient, the relaxation time and the melt viscosity with the molecular weight.[39–41] These studies were performed with different methods, and in particular, with photon correlation spectroscopy and the neutron spin echo technique.[43,49] The experimental conditions were chosen in such a way that the polymer probe is visible to the incident radiation and the polymer matrix is invisible. Moreover, the probe is infinitely dilute in such a way that its chains do not interact with each other and one effectively measures the single chain diffusion coefficient. This subject is well documented in the literature.[3,14,29,43–49] Here, we are interested in systems fulfilling the ZAC since, in this,condition, it is possible to have direct access to the interdiffusive process and to study the effect of incompatibility on the relative motion of chains of different species. Before examining this problem in more detail, we first present some general considerations on the dynamic scattering of multicomponent polymer systems.

Dynamical properties can be investigated starting from the generalized Langevin equation (GLE) for the monomer concentration fluctuation $\delta c(q,t)$:[29]

$$\partial \delta c(q,t)/\partial t + \Omega(q)\delta c(q,t) - \int_0^t \mathrm{d}u\ \Phi(q,t-u)\delta c(q,u) = f(q,t), \tag{95}$$

$\delta c(q,t)$ is the fluctuation of the monomer concentration from the equilibrium mean value c_0:

$$\delta c(q,t) = c(q,t) - [c_0/V]\delta(\boldsymbol{q})$$

where $\delta(\mathbf{q})$ is the Dirac delta function and V the volume of the system. One has:

$$\delta c(q,t) = \sum_{\text{all monomers } j} e^{iq.rj}. \tag{96}$$

A similar equation can be obtained for the intermediate scattering function $S(q,t)$:

$$\partial S(q,t)/\partial t + \Omega(q)S(q,t) - \int_0^t du\ \Phi(q,t-u)S(q,u) = 0 \tag{97}$$

where $S(q,t)$ is the two times auto-correlation function for the concentration fluctuations:

$$S(q,t) = < \delta c(q,t)\delta c^*(q,0) > . \tag{98}$$

In eqn (95) and eqn (97), $\Omega(q)$ represents the first cumulant, $\Phi(q,t)$ the memory function and $f(q,t)$ a random noise. The memory function

$$\Phi(q,t) = < f(q,t)f^*(q,0) >$$

is two times the autocorrelation function for the random noise. This function is extremely difficult to calculate and only for a few cases can one calculate $S(q,t)$ including memory effects.[50–54] Fortunately, the initial decay of $S(q,t)$ defined by the first cumulant $\Omega(q)$ is often sufficient to characterize the dynamics of the system and analyse the quasi-elastic light scattering data from polymer systems. This is true at least in the early stages of the relaxation of the concentration fluctuations described by the time evolution of $S(q,t)$:

$$\partial S(q,t)/\partial t + \Omega(q)S(q,t) \approx 0. \tag{99}$$

The time evolution of the mean concentration $c_m(q,t)$ also satisfies a similar equation. We shall discuss later how the first cumulant $\Omega(q)$ can be useful for the study of the dynamical properties of polymer mixtures.

For multicomponent mixtures, the above equations remain valid, but they must be written in matrix form. Let us first consider eqn (99) which we write for the intermediate scattering matrix $\mathbf{S}(q,t)$. Its solution gives the partial dynamic structure factors $S_{ij}(q,t)$ as a function of the first cumulant $\Omega(q)$ and the static structure matrix $\mathbf{S}(q) = \mathbf{S}(q,t = 0)$. It becomes a straightforward problem to characterize the dynamics of multicomponent mixtures within the mean field approximation neglecting memory effects if one knows $\Omega(q)$. This matrix is defined in terms of the mobility matrix $\mathbf{M}(q)$ and the structure matrix $\mathbf{S}(q)$ as:

$$\Omega(q) = q^2 K_B T \mathbf{M}(q)\mathbf{S}(q)^{-1}. \tag{100}$$

The knowledge of the mobility matrix $\mathbf{M}(q)$ requires the choice of a dynamical model. Using the Oseen tensor description or equivalently, the Kawasaki mode coupling model, one can write the elements of the matrix $\mathbf{M}(q)$ as:[55]

$$M_{ij}(q) = \delta_{ij}\varphi_i/\zeta_i + 1/(4\pi^2\eta)\int_0^\infty dk f(k/q)S_{ij}(k) \tag{101}$$

where δ_{ij} is the kronecker delta function, ζ_i the friction coefficient of monomer i, and $f(x)$ the so-called Kawasaki function:[55,56]

$$f(x) = x^2\{[(x^2+1)/2x]\log|(x+1)/(x-1)| - 1\}. \tag{102}$$

This result is written neglecting the screening of the hydrodynamic interactions. Should this effect become significant, which would be the case if the concentration is high and the overlapping of the polymers strong, then $f(x)$ has to be modified. A possible modification is to use the screened Oseen tensor and instead of $f(x)$, one would have to introduce a function of the two variables $f(x,y)$ with $x = k/q$ and $y = 1/q\xi$:

$$f(x,y) = x^2\{[(x^2+1+y^2)/4x]\log[(x+1)^2+y^2]/[(x-1)^2+y^2]-1\} \tag{103}$$

where ξ is the hydrodynamic screening length which, to a good approximation, can be identified with the static correlation length introduced earlier. Borsali *et al.*[57] used this model of hydrodynamic screening to study the reduced viscosity of polyelectrolytes and its variation with polymer concentration. Richter *et al.*[58], and Rooby and Joanny[59] used arguments based on a local q-dependent viscosity to study polymer solution dynamics in the presence of hydrodynamic interactions. Their model of q-dependent viscosity is consistent with the screening model invoked here.

2.2.2. *Dynamic scattering functions*

In the case of a multicomponent mixture, the dynamic scattering intensity $I(q,t)$ can be written as:

$$I(q,t) = v^T \mathbf{S}(q,t) v. \tag{104}$$

The partial dynamic structure factors $S_{ij}(q,t)$ should be obtained from the resolution of the approximate Langevin eqn (99) or its counterpart in the matrix form neglecting memory effects:

$$\boldsymbol{S}(q,t) = \mathrm{e}^{-\Omega(q)t}\mathbf{S}(q). \tag{105}$$

If the mixture is made of two polymer species A and B and a solvent, this equation is easily solved and the result gives a bimodal distribution function:

$$S_{ij}(q,t) = A_{ij}\mathrm{e}^{-\Gamma_f t} + A'_{ij}\mathrm{e}^{-\Gamma_s t}, \tag{106}$$

where $\Gamma_{f,s}$ are the frequencies of the fast and slow modes and are given by the eigenvalues of $\Omega(q)$:

$$\Gamma_{f,s} = \Omega_{\mathrm{av}} \pm (\Omega_{\mathrm{av}}^2 - \Delta\Omega)^{1/2}, \tag{107}$$

$$\Omega_{\mathrm{av}} = (\Omega_{11}+\Omega_{22})/2 \qquad \Delta\Omega = \Omega_{11}\Omega_{22} - \Omega_{12}\Omega_{21}. \tag{108}$$

The amplitudes of these modes A_{ij} and A'_{ij} are expressed in terms of the partial structure factors and eigenfrequencies as:

$$A_{\mathrm{aa}} = [S_{\mathrm{aa}}(\Omega_{\mathrm{bb}} - \Gamma_{\mathrm{f}}) - \Omega_{\mathrm{ab}}S_{\mathrm{ba}}]/(\Gamma_{\mathrm{s}} - \Gamma_{\mathrm{f}}) \qquad A'_{\mathrm{aa}} = S_{\mathrm{aa}} - A_{\mathrm{aa}}, \tag{109}$$

$$A_{\mathrm{ab}} = [S_{\mathrm{ab}}(\Omega_{\mathrm{aa}} - \Gamma_{\mathrm{f}}) - \Omega_{\mathrm{ab}}S_{\mathrm{bb}}]/(\Gamma_{\mathrm{s}} - \Gamma_{\mathrm{f}}) \qquad A'_{\mathrm{ab}} = S_{\mathrm{ab}} - A_{\mathrm{ab}}. \tag{110}$$

A_{bb} and A_{ba} can be deduced from these equations by interchanging the indices a and b, and $S_{\mathrm{ab}}(q) = S_{\mathrm{ba}}(q)$. As already pointed out, early experiments of quasielastic light scattering from ternary mixtures were made with compatible mixtures where one of the two polymers was visible and its concentration very small. Their main motivation was to understand the mechanism of chain diffusion in concentrated solutions (or in bulk) and to test whether the

predictions of the reptation model proposed by de Gennes could be verified. In this case, the scattering signal is proportional to $S_{aa}(q,t)$ which in general shows both the fast and the slow processes. However, the amplitude of the fast mode in this case is too small to be resolved from the autocorrelation function and one usually observes a single exponential decay corresponding to the slow mode:

$$S_{aa}(q,t) \approx S_{aa}(q)e^{-\Gamma s^t}. \tag{111}$$

However, since this case is not a major case in our investigation of mixtures under the ZAC condition, we leave the problem at this stage and turn to the discussion of the dynamics of mixtures satisfying the ZAC.

2.2.3. *Dynamic scattering under the ZAC*

The dynamical correlation function under the ZAC is also characterized by a single exponential decay function describing the slow mode. The study of the relaxation in time can be conducted in a similar way as in the static scattering. One finds that for incompressible mixtures, the dynamic scattering intensity $I(q,t)$ can be split into three terms:

$$I(q,t) = [(v_a - v_s)x + (v_b - v_s)(1-x)]^2 S_{cc}(q,t) + (v_a - v_b)^2 S_{xx}(q,t)$$
$$+ 2[(v_a - v_s)x + (v_b - v_s)(1-x)](v_a - v_b)S_{xc}(q,t). \tag{112}$$

The first term in the right hand side of this equation describes the relaxation of the concentration fluctuations, the second is related with the composition fluctuations and the third term is the coupling between these two fluctuations. From an experimental point of view, one can have access to these contributions separately by choosing the "optical" conditions properly. In the absence of contrast between the two polymers, one has $v_a = v_b$ and the second and last terms in eqn (112) vanish. The scattering in this case is entirely due to the concentration fluctuations represented by $S_{cc}(q,t)$. On the other hand, if the average contrast $(v_a - v_s)x + (v_a - v_s)(1-x)$ is zero, the first and last terms in eqn (112) vanish and the scattering signal is entirely due to the composition fluctuations. In the case of a 50/50 symmetrical mixture, $x = 1/2$, the coupling between concentration and composition fluctuations disappears and both $S_{cc}(q,t)$ and $S_{xx}(q,t)$ decay following single exponentials. One finds that these exponentials decay in different time scales and correspond to different mechanisms. For example:

$$S_{cc}(q,t) = McP(q)/[1 + 2A_2McP(q)]e^{-\Gamma_C t} \tag{113}$$

represents the relaxation of the fluctuations in the local polymer concentration. The other process is represented by the function $S_{xx}(q,t)$:

$$S_{xx}(q,t) = McP(q)/[1 - \chi McP(q)/2]e^{-\Gamma_I t} \tag{114}$$

which describes the relaxation of the fluctuations in the local polymer composition.

In order to represent these processes, we have introduced a new notation and identified the fast process which is related with the concentration as the cooperative mode, and the slow process which is related to the composition as the interdiffusive mode. The amplitudes of these processes are:

$$S_C(q) = S_{cc}(q, t=0) = S_{cc}(q) = N\varphi P(q)/([1 + (v + \chi/2)N\varphi P(q)], \tag{115}$$

$$S_I(q) = S_{xx}(q, t=0) = S_{xx}(q) = N\varphi P(q)/[1 - \chi N\varphi P(q)/2]. \quad (116)$$

The relaxation frequencies of these modes can be expressed as sums of two different contributions. The first one describes the short range frictional forces of the Rouse dynamics and the second one describes the long range hydrodynamic interaction. Assuming that the friction coefficients are equal, $\zeta_a = \zeta_b = \zeta$, one finds:

$$\Gamma_C(q) = q^2 kT\varphi/[\zeta S_C(q) + 1/(4\pi^2\eta)\int_0^\infty dk f(k/q, q\xi)S_C(k) \quad (117)$$

and

$$\Gamma_I(q) = q^2 kT\varphi/[\zeta S_I(q)] + 1/(4\pi^2\eta)\int_0^\infty dk f(k/q, q\xi)S_I(k) \quad (118)$$

where the function $f(x,y)$ is defined in eqn (103).

2.2.4. *Critical slowing down*

When the temperature of the mixture approaches its critical value, the amplitude and wavelength of fluctuating modes increase very fast and their relaxation slows down considerably. The amplitude and range of these fluctuations can be studied by static light scattering as we have seen earlier. To complete the analysis of critical mixtures, one could also examine the dynamics using either photon correlation or neutron spin echo techniques. Recently there has been a growing interest concerning the critical slowing down of composition fluctuations of homopolymer blends, for block copolymers and ternary mixtures of polymers and a solvent.[36,60–71] A major question which arises from these studies is to know whether one observes a single or two critical relaxation modes and to understand what physical processes they represent. This question will be addressed in more detail below.

3. EXPERIMENTAL EXAMPLES

In this section, we discuss some examples of data obtained by light, neutron or X-ray scattering techniques on polymer blends and block copolymers in solution under the ZAC. We do not pretend to present a complete review of all the systems investigated, and we shall make a selection of the systems which, in our opinion, represent examples that best illustrate the theoretical formalisms discussed in the first part of this paper and which serve our purpose of focusing on systems that fulfill the ZAC condition.

3.1. *PS/PMMA/bromobenzene*

To our knowledge, this mixture is the first one to be chosen for investigating static properties using light scattering under the ZAC. This investigation was reported by Fukuda *et al.*[15] who considered several mixtures characterized by different concentrations and molecular weights. Although eqn (46) was obtained in the dilute limit, it was nevertheless used for determining χ_{ab} by light scattering for PS/PMMA/bromobenzene over a wide range of concentrations. A similar procedure has been used by Ould-Kaddour and Strazielle[72–74] for other mixtures under the ZAC. Some results are provided in Fig. 1. This figure shows the variation

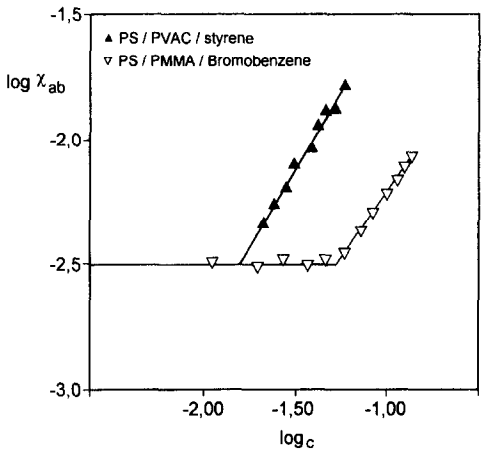

Fig. 1. The variation of log χ_{ab} as a function of logc for two ternary mixtures ▲: PS/PVAC/styrene;[72,73] ▽: PS/PMMA/bromobenzene.[15]

of χ_{ab} as a function of concentration c in a log–log plot for PS/PMMA/bromobenzene (open triangles ▽) and PS/PVAC(polyvinylacetate)/styrene (filled triangles ▲). In both systems, one observes the existence of a crossover at a certain concentration where the variation of χ_{ab} changes qualitatively. This crossover concentration depends on the mixture under consideration and has been found to be much higher than the overlap concentation c^*. This figure shows that below the crossover concentration, the interaction parameter χ_{ab} remains essentially constant but above this concentration, the interaction parameter increases with c but not linearly. This increase follows a power law which is slightly system dependent. Examples of these power laws are:[72–74]

$$\chi_{ab} \sim c^{0.53} \quad \text{for PS/PMMA/bromobenzene}$$
$$\chi_{ab} \sim c^{0.6} \quad \text{for PS/PMMA/toluene}$$
$$\chi_{ab} \sim c^{0.7} \quad \text{for PS/PVAC/styrene.}$$

Using scaling arguments, de Gennes[14] predicted the power law $\chi_{ab} \sim c^{0.25}$ whereas renormalization group theory calculations[13,39,41,75] gave $\chi_{ab} \sim c^{0.3}$. One observes that the experimental exponent is systematically higher than the theoretical predictions. This observation was first made by Fukuda *et al.*[15] and later by Ould-Kaddour and Strazielle.[74] Moreover, the interaction parameter χ_{ab} depends on the molecular weight and this dependence seems also to follow a power law. This power law behavior has been examined for several mixtures fulfilling the ZAC and in particular for PS/PMMA/bromobenzene. Figure 2 shows a plot of $\log[\Delta A_{2ab} \approx \chi_{ab}]$ with respect to log M for several mixtures. Consistent with the renormalization group theory result of eqn (92), one observes a linear decrease indicating the power law:

$$\chi_{ab} \sim M^{-0.45}. \tag{119}$$

The concentration at which phase separation occurs through spinodal decomposition in these ternary mixtures is denoted c_K. This critical concentration is sensitive to the average molecular weight of the polymers M. In Fig. 2, we also represent the variation of log c_K as a

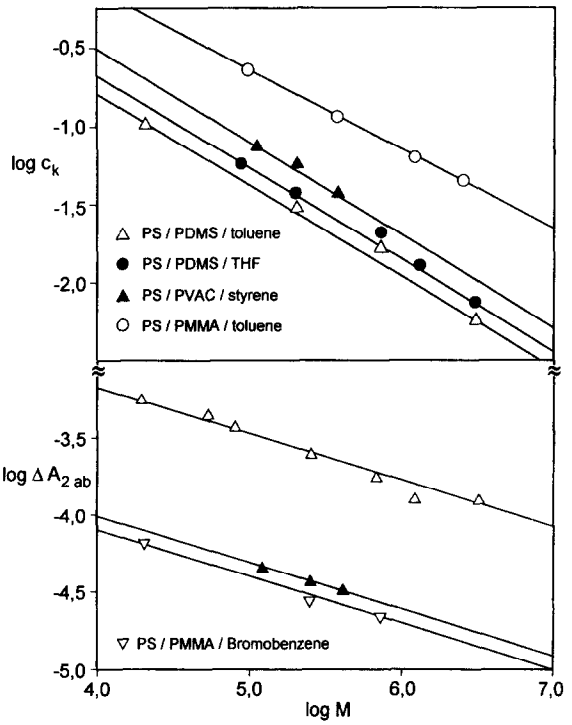

Fig. 2. The variations of log c_k (top) and logΔA_{2ab}~logX_{ab} (bottom) as a function of log M for five different ternary mixtures.[15,72–74]

function of log M for different systems satisfying the ZAC. Ould-Kaddour and Strazielle[73] reported the following power law obtained by static light scattering:

$c_k = 44.6 \times M^{-0.58}$	PS/PDMS/THF
$c_k = 43.6 \times M^{-0.59}$	PS/PDMS/toluene
$c_k = 227 \times M^{-0.61}$	PS/PMMA/benzene
$c_k = 81.7 \times M^{-0.62}$	PS/PVAc/styrene.

Equation (94) shows that these power laws are consistent with the renormalization group theory calculation.

Besides the investigation of Fukuda *et al.*[15] on PS/PMMA/bromobenzene, the only further study of this system by light scattering was reported recently by Seils *et al.*[36] These authors reported elastic and quasi-elastic light scattering measurements under the ZAC, at a fixed concentration and composition and with temperatures varying between 30 and 2°C. This mixture shows an upper critical solution temperature and, in the vicinity of 2°C, it phase separates via spinodal decomposition. Static and dynamic measurements show two distinct regimes of temperature. Above 7°C, the mean field model is found to describe the data quite well. Below 7°C, substantial deviations from this mean field description are observed, in particular for the prediction of the critical exponents. The procedure of extrapolating the high temperature data to the point where $1/I(q = 0) = 0$ gives a mean field estimate of the critical temperature T_0 which does not seem to be correct. This means that the mean field description

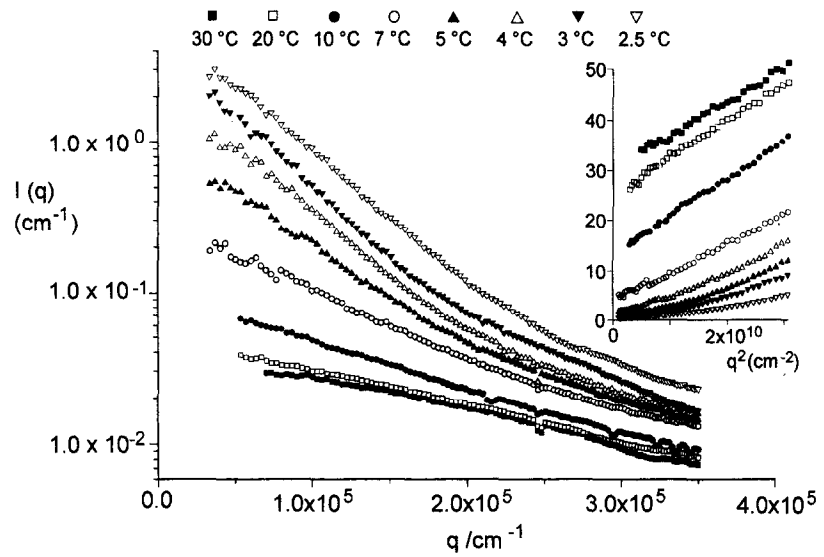

Fig. 3. The variation of $I(q)$ as a function of q for PS/PMMA/bromobenzene. Curves from bottom to top correspond to decreasing temperatures.[36] The insert represents an Orsntein–Zernick plot of the same data in the lower range of q.

fails to represent the behavior of the system near its critical temperature where the fluctuations are very strong and the scattering is substantially enhanced. This enhancement of $I(q)$ when the temperature decreases is more significant in the small q range since the fluctuating modes in the long wavelength regime dominate the scattering.

In the experiments of Seils *et al.*,[36] it is found that $I(q)$ should be split into two parts: a critical contribution which is sensitive to temperature and a non-critical part which remains essentially constant. We will refer to this constant value as the background component. The critical component dominates the scattering in the vicinity of T_c and, therefore, it is this part which is important if one wants to extract the scaling properties or the critical exponents governing the scattering signal. Following the procedure used in the case of low molecular weight liquid mixtures, Seils *et al.*[36] suggested subtracting the constant background from the total signal to analyze the critical behavior. This background turns out to be more accurately evaluated from the quasi-elastic data. It is obtained from the amplitude of the faster mode emerging in the autocorrelation function at 7°C. This is the fastest of the two modes characterizing the time relaxation of the auto correlation function at 7°C and below and which seems to remain essentially unchanged with temperature. The background is subtracted from the signal to isolate the critical component reflecting the order parameter (or composition) fluctuations.

Figure 3 describes the variation of the scattered intensity as a function of q at various temperatures ranging from 2.5 to 30°C. It shows clearly the sharp increase in the scattering as T decreases, especially in the low q range. The insert in this figure gives the same results in a different representation. It shows $I(q)$ as a function of q^2 in the lower q range, which is more relevant for the study of the critical behavior. One observes that the scattered intensity deviates from the standard Ornstein–Zernick form as the temperature approches the critical value. This makes the extraction of the correlation length ξ somewhat ambiguous. Letting

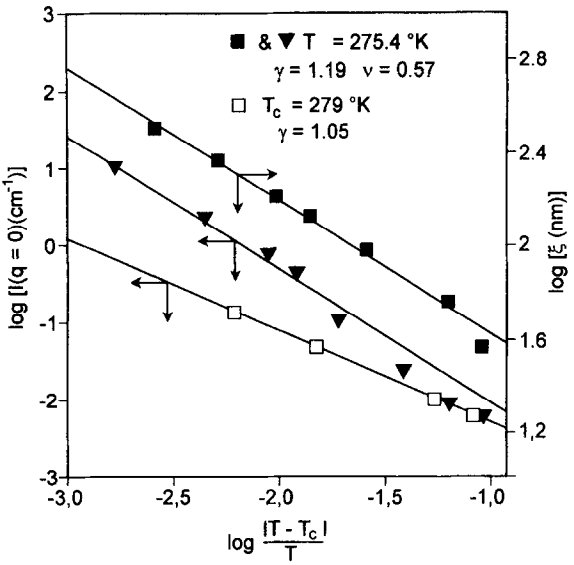

Fig. 4. The variations of $\log I(q = 0)$ and $\log \xi$ as a function of $\log \epsilon$ where ϵ is defined with respect to T_0, the mean field critical temperature (□) or T_c the Ising critical temperature (▼, ■).[36]

$q = 0$, one obtains the variation of the forward scattered intensity as a function of T and this variation can be used to extract important information on the critical behavior of the thermodynamic properties of the mixture. Considering the critical part of the scattering intensity at $q = 0$ as a function of T, one finds that, in the temperature range above 7°C, the data follow quite well the mean-field description given in the early part of this chapter.

As the critical temperature is approched, strong deviations from this picture are observed. This was the case for polymer blends[60–65] and for ternary mixtures in the presence of a low molecular weight solvent.[36,69–71] The inverse forward scattering intensity at $1/I(q = 0)$ decreases linearly with $1/T$ in the upper temperature range and the extrapolation of this line gives a mean field estimate of the critical temperature T_0. But this estimate is found to differ substantially from the real critical temperature at which the forward scattering intensity effectively diverges. This temperature T_c is sometimes referred to as the Ising critical temperature.[36,60–71] The exponents γ and ν governing the critical behavior of the forward scattering intensity $I(q = 0) \sim \varepsilon^{-\gamma}$ and the correlation length $\xi \sim \varepsilon^{-\nu}$ near T_c have values different from the mean field predictions $\gamma = 1$ and $\nu = 1/2$.

Fig. 4 shows the data obtained by Seils *et al.*[36] on PS/PMMA/bromobenzene representing $\log I(q = 0)$ and $\log \xi$ as a function of $\log \varepsilon$. The filled squares and triangles are data for the intensity and correlation length obtained by defining ε in terms of the Ising critical temperature $\varepsilon = |T - T_c|/T$, respectively. The open squares are data for the intensity where ε is defined in terms of the mean field critical temperature T_0. The scaling behavior of the inverse scattering intensity shows a transition from the mean field-like exponent $\gamma = 1.05$ in the upper temperature range to the Ising-like exponent 1.19 near T_c. If one defines the reduced temperature as $\varepsilon = |T - T_0|/T$ (open squares in Fig. 4), one finds that $\gamma = 1.05$ is very close to the mean field prediction in the whole range of temperature covered in these experiments. For

pure blends, Meier *et al.*[65] observed that if one defines ε in terms of the mean field critical temperature, one observes a transition in the exponent from mean field-like to Ising-like exponents. On the other hand, if one defines ε in terms of the Ising critical temperature one observes the Ising exponent at all temperatures. This means that the results of Seils *et al.*[36] are in disagreement with those of Meier *et al.*[65] and one may be tempted to attribute such a discrepancy to the changes introduced by the low molecular weight solvent. However, this does not seem to be the case since similar discrepancies are also observed with the data of Miyashita *et al.*[69,70] on the ternary mixture PS/PMMA/deuterated benzene.

It is interesting to note that, although comprised of the same type of polymers as the one investigated by Seils *et al.*,[36] the latter system shows significant differences. The first major difference concerns the phase diagram which has a lower critical solution temperature (LCST) whereas the blend considered by Seils *et al.*[36] of similar polymers in bromobenzene is characterized by an upper critical solution temperature (UCST). Miyashita *et al.*[69,70] were able to analyze their data using a procedure similar to the one adopted previously by Stepanek *et al.* and by Meier *et al.*[60,61,63,65] for pure blends. They were able to characterize the scaling behavior of the forward scattering intensity without having to subtract the background contribution and found the Ising exponent $\gamma = 1.23$. With regards to the correlation length, they observed that the variation of the scattered intensity as a function of q^2 was consistent with the standard Ornstein–Zernicke plot. This allowed them to extract the correlation length ξ and find that its scaling behavior is also governed by the Ising exponent $\nu = 0.63$.

In more recent work, Miyashita and Nose[69,70] studied in more detail the critical behavior of PS/PMMA/deuterated benzene and PS/poly(2-chlorostyrene)/deuterated benzene with different indices of polymerization and different concentrations. In addition to the scaling behavior of the forward scattering intensity and the correlation length in the crossover region, they analyzed the scaling behavior of the Ginzburg number using the universal crossover function obtained by Anisimov and Kiselev[76] from the renormalization group theory. This means that the data for PS/PMMA/deuterated benzene reported by Miyashita and Nose did not seem to show the same complexity in the scattering behavior observed by Seils *et al.*[36] in the presence of bromobenzene. It is however worth pointing out that the increments of refractive indices of both PS and PMMA in deuterated benzene are finite implying that both polymers contribute to the scattering signal. One would expect to have not only a contribution from the concentration fluctuations but also significant scattering due to the coupled fluctuations of concentration and composition order parameters. It is not clear that these contributions should be neglected over the whole range of temperatures and concentrations covered in the experiments of Miyashita and Nose in spite of the fact that near the critical temperature, one would expect the critical composition fluctuations to dominate the scattering signal.

In addition to the static light scattering investigation on PS/PMMA/bromobenzene, Seils *et al.* performed quasielastic light scattering experiments in the same conditions as those reported earlier. This combined analysis of the static and dynamic properties is very useful because it enables one to have a better insight into the peculiarities of this mixture when the critical temperature is approched. Consistent with the subtleties observed in the static data, other subtleties were found in the dynamic data in similar conditions. For example, measurements of the intermediate scattering function revealed that between 30 and 7°C, the dynamics are governed essentially by a single mode describing a standard relaxation of the fluctuations in the composition of the A and the B polymers. The decay frequency of this mode is essentially proportional to q^2 and its diffusion coefficient D^1 is consistent with the

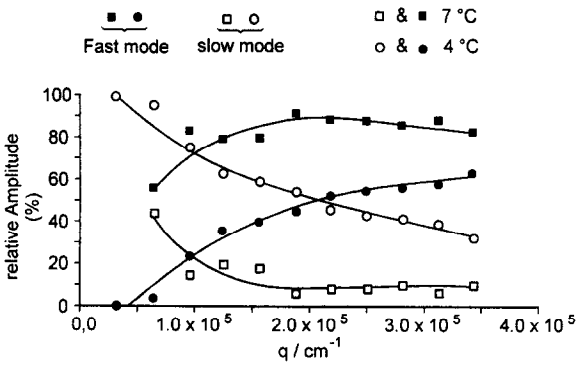

Fig. 5. The variations of the relative amplitudes of the fast and slow modes as a function of q at two different temperatures. Measurements made by quasielastic light scattering on PS/PMMA/bromobenzene.[36]

RPA predictions given in eqn (118) where $D_I = \Gamma_I/q^2$. At 7°C and below, the dynamic scattering function shows a double exponential behavior indicating that at least two relaxation processes characterize the dynamics of the mixture near the critical temperature. The fast mode is essentially the same as the one observed at higher temperatures and seems to remain essentially unchanged with T. The slower mode emerging at 7° undergoes a considerable slowing down as the temperature approches 2°C. Whereas the relaxation frequency of the fast mode has a q^2 behavior at all temperatures, the frequency of the slow mode shows a crossover from q^2 to q^3 behaviors characteristic of mode coupling effects.

In Fig. 5, the variations of the relative amplitudes of the fast (■ at 7°C and ● at 4°C) and slow (□ at 7°C and ○ at 4°C) modes at the two temperatures 7 and 4°C are represented. At 7°C, one observes that in the lowest q range, the two amplitudes are comparable but the amplitude of the slow mode quickly decays to zero as q increases. The fluctuations with long wavelengths dominate the scattering as the temperature decreases and the fluctuations become weaker as one looks at shorter scales. At 4°C, the relative amplitude of the slow mode is almost 100% in the lower q range and decreases only moderately as q increases. Likewise, the relative amplitude of the fast mode increases moderately with q indicating that the contribution of the fast mode is more significant at short length scales. Seils *et al.*[36] analyzed the first cumulant $\Gamma(q)$ in the range below 7°C and observed that it has a q^2 behavior describing the usual diffusive process. As the temperature is lowered below 7°C, they observed a transition from $\Gamma \sim q^2$ to $\Gamma \sim q^3$ behavior indicating a crossover due to long range mode coupling effects. This behavior is visualized in Fig. 6 where we have chosen to represent the normalized mobility ηM_{xx} or:

$$\eta M_{xx} = \Gamma(q) S_{xx}(q)/[q^2 K_B T] = \eta\mu(q) = (1/4\pi^2) \int_0^\infty dk f(k/q) S_{xx}(k). \tag{120}$$

From this equation, one expects that $\eta\mu(q)$ increases at small temperatures and small qs due to the modes coupling effects, the long range fluctuations and the viscosity enhancement. The continuous lines represent eqn (120) which is the theoretical prediction obtained from mode coupling theory. The insert shows the variation of Γ/q^3 as a function of q in the same temperature range. At low temperatures, this figure shows that the mode coupling behavior $\Gamma \sim q^3$ dominates in the whole range of q whereas in the upper temperature region, the q^3

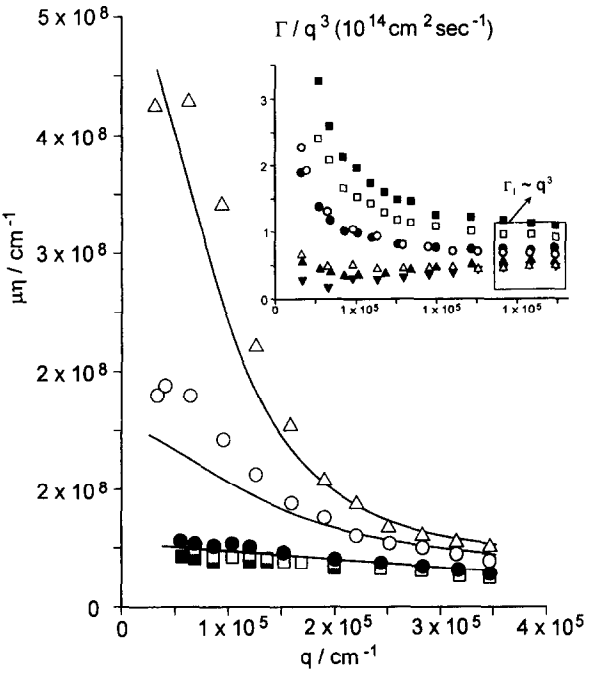

Fig. 6. The variation of the product mobility times viscosity as a function of q for PS/PMMA/bromobenzene at different temperatures ranging from 30 to 2.5°C. The insert represents the normalized first cumulant Γ/q^3 for the same data.[36]

behavior appears in the high q range only. The upturn in the curves is the signal for a transition to a purely diffusive process where $\Gamma \sim q^2$.

Yajima *et al.*[71] performed quasi-elastic light scattering on ternary solutions of d-PS/PB(polybutadiene)/DOP. They observed two relaxation modes in the decay of the intermediate scattering function in the vicinity of the critical temperature. Their data show that the relaxation frequencies of the two modes have a q^2-dependence and both slow down critically. However, no mode coupling q^3 behavior was reported in these data. The fact that both modes are diffusive and subject to critical slowing down indicates a major discrepancy with known results. These controversies indicate that there is a need for more work along these lines to elucidate the effects of polymer interactions and the changes in the dynamics of polymer mixtures due to the presence of low molecular weight solvents.

3.2. *PS/PDMS/solvent*

These polymers are characterized by a relatively high degree of incompatibility meaning that the interaction parameter χ_{ab} should show stronger effects on the thermodynamic, structural and dynamic properties as revealed, for example, by the scattering techniques. The static scattering properties of PS/PDMS in different solvents have been studied in detail by Ould-Kaddour and Strazielle.[72–74] These authors have chosen particular solvents that fulfill the ZAC such as toluene, chloroform, carbone tetrachloride, cyclohexane and styrene. The results showing the variation of $Kc/I(q = 0)$ as a function of c for these mixtures are collected in

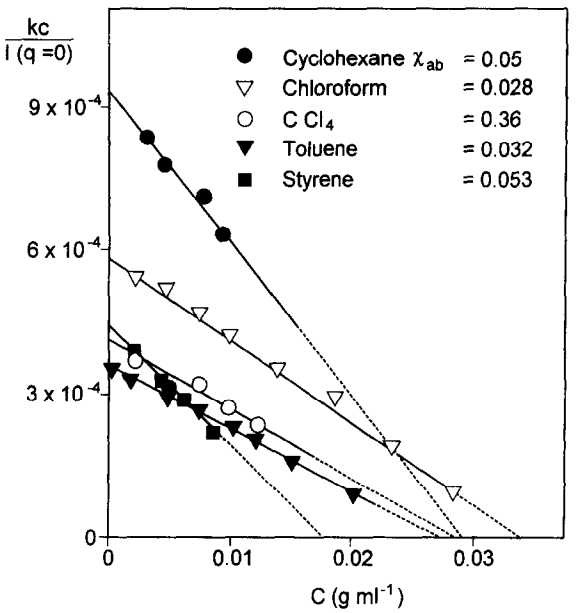

Fig. 7. The variation of $Kc/I(q=0)$ as a function of c for the ternary mixture PS ($M=2.3\times10^5$)/PDMS ($M=28\times10^5$)/solvent at 25°C. Different symbols correspond to different solvents as indicated in the figure.[72–74]

Fig. 7 for polymers of molecular weights $M_{PS} = 2.3 \times 10^5$ and $M_{PDMS} = 2.8 \times 10^5$. All the plots show that $Kc/I(q = 0)$ decays linearly with concentration c and from the slope, one can deduce the interaction parameter χ_{ab} using the RPA result:[72]

$$K'c_T/\Delta I(q=0) = A + \chi_{ab}BA^2c_T \tag{121}$$

where the subscripts a and b stand for PS and PDMS, respectively and the other quantities are $c = c_a + c_b$ the total concentration, $y = c_a/(c_a + c_b)$ the composition of PS and:

$$A = [(v_a - v_s)^2 M_a y + v_b^2 M_b (1-y)]^{-1}$$

$$B = 2(v_a - v_s)(v_b - v_s) M_a M_b y(1-y) v_{0a} v_{0b}/v_{0s}.$$

The values of the interaction parameter deduced from this analysis at a fixed temperature vary from 0.028 to 0.053 depending on the solvent. This result is surprising since one would expect that under the ZAC, the interaction parameter would be independent of the solvent. This could be explained however by the fact that the ZAC condition is not strictly satisfied and that the two polymer–solvent interaction parameters are not rigorously equal and some preferential adsorption takes place.

In their quasielastic scattering measurements on a symmetrical mixture of PS/PDMS/toluene under the ZAC, Giebel *et al.*[77] observed a single relaxation mode in the time evolution of the intermediate scattering function. From the analysis of their data, they concluded that this mode should correspond to the interdiffusive process consistent with the RPA prediction.

3.3. *PMMA/PDMS/chloroform*

This is another example of incompatible mixtures which can be investigated by scattering experiments under the ZAC. Giebel *et al.*[78,79] performed QELS experiments on such mixtures under the ZAC and considered a concentration range roughly between c^* and $5c^*$ at room temperature. At $5c^*$, the mixture remains homogeneous in a single phase and the critical concentration c_K is slightly above $5c^*$. QELS measurements were made using different polymer compositions comprised between 0 and 100%. The results indicate that the auto-correlation function decays following a single exponential in the composition range between 0.3 and 0.7. Outside this range, a second fast mode emerges and its behavior is characteristic of the relaxation of the concentration fluctuations. The auto-correlation function shows a bimodal distribution and the relative amplitude of the cooperative mode $a_C/(a_C + a_I)$ is displayed in Fig. 8 as a function of x_{PMMA}, the composition in PMMA of the blend. The dotted line represents the theoretical prediction based on the RPA and the squares are the data. The two inserts in this figure show typical relaxation time distributions obtained from Contin analysis of the auto-correlation functions. The insert on the right hand side is an example corresponding to values of x for which there are two modes and the insert on the left hand side represents an example of the intermediate region of x for which only the slow interdiffusive mode appears.

It is interesting to note that this method allows one to extract important information on static and dynamic properties. It has been suggested as a method for extracting the values of the interaction parameter χ_{ab} and the single chain diffusion coefficient D_s.[79–81] In a previous paper,[79] the self-diffusion coefficient D_s was deduced from the data available in the literature assuming the stretched exponential model of Phillies.[82] This made possible the measurement of χ_{ab} without any adjustable parameter. Debrieres *et al.*[83] studied mixtures of succinoglican + dextran in aqueous solutions by QELS for different concentrations and compositions. The

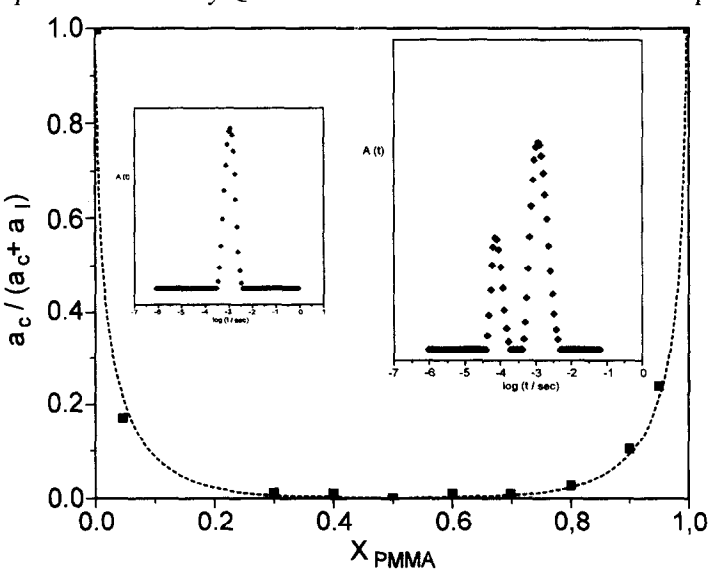

Fig. 8. The variation of the relative amplitude of the cooperative mode as a function of the composition of PMMA for the mixture PMMA/PDMS/chloroform. The inserts represent the results for two compositions obtained from the Contin analysis.[78,79,81]

data were analyzed using the formalism described in the theoretical section keeping the interaction parameter χ_{ab} and the single chain diffusion coefficient D_s as adjustable parameters. Their data were found to fit quite well with the theoretical prediction of the RPA and the fit was used to extract the values of χ_{ab} and D_s. Wang *et al.*[84] also used the same RPA formalism to describe their light scattering results from ternary mixtures of two homopolymers and a solvent. Their observation was that in the absence of intermolecular hydrodynamic interactions where $M_{ab} = M_{ba} = 0$, the formulae simplify greatly and the data analysis becomes much more convenient. This simplification was possible regardless of the two polymers and not only for the case of mixtures fulfilling the ZAC condition.

3.4. *PS/PDMS/PMMA/toluene*

The knowledge of the properties of quaternary mixtures of polymers in solvents can be important from a fundamental point of view since this is a good example of a multicomponent mixture where the theoretical formalism such as the one presented earlier can be tested. It is also useful for practical purposes such as in the case of membranes where one usually deals with two polymers and two solvents with different thermodynamic properties. Static and dynamic scattering studies on ternary mixtures of PS/PDMS/toluene under the ZAC are known and it was interesting to explore the effects of a third polymer on these properties. An interesting case is one where the third polymer has the same index of refraction as the solvent such as PMMA and therefore does not contribute directly to the scattered light. An investigation of this system using elastic and quasielastic light scattering was reported by Strazielle *et al.*[31–33] over a wide range of concentrations and for different molecular weights. Figure 9 displays the variation of the normalized scattering intensity $I(q = 0,\varphi = 0)/I(q = 0,\varphi)$ as a function of the volume fraction of PS and PDMS, $\varphi = \varphi_{PS} + \varphi_{PDMS}$, for five systems characterized by different concentrations of PMMA. One can analyze these data either by using a pseudo-binary picture assuming that the PMMA introduces modifications of the properties of the solvent matrix. A more realistic theoretical scheme is the one in which PMMA, although invisible to the incident radiation, is still considered as a full component and formulae are derived where its properties are explicitly included. This formalism is described in the theoretical part of this paper and an apparent interaction parameter χ_{app} is derived in terms of the concentrations, the molecular weights, and the other polymer–polymer and polymer–solvent interaction parameters. The continuous lines represent the theoretical predictions as displayed by eqn (60) and eqn (61) and the values are found elsewhere.[33] With regards to the quasielastic light scattering data, one would expect a multimodal autocorrelation function for such a multicomponent mixture. Surprisingly enough, the analysis of the autocorrelation function by standard methods such as the Contin algorithm revealed that the autocorrelation function presents a single exponential mode. The relaxation frequency of this mode is found to be proportional to q^2 over the entire experimental q range. The insert of Fig. 9 gives the corresponding diffusion coefficient D_I for the five concentrations of PMMA. The extrapolation of D_I to $\varphi = 0$ gives the self-diffusion coefficient D_s which depends upon the volume fraction of PMMA. It is interesting to note that the curves representing the normalized diffusion coefficient D_I/D_s as a function of φ coincide with those of $I(q = 0, \varphi = 0)/I(q = 0,\varphi)$ for the five concentrations investigated. This means that hydrodynamic interactions are not important, consistent with the theoretical scheme where the RPA and the Rouse model are combined.

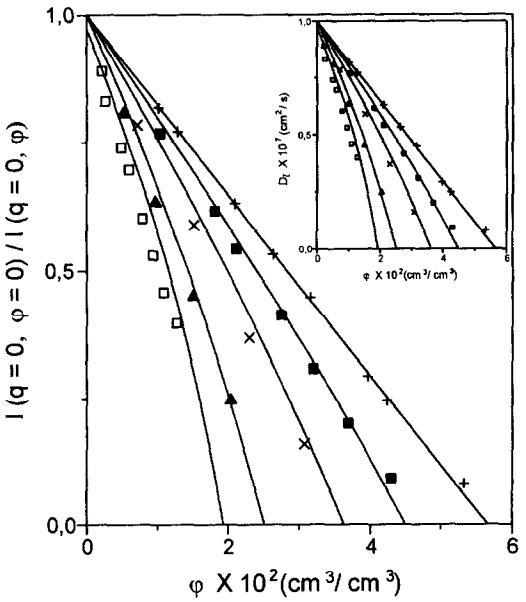

Fig. 9. The variation of the normalized scattering intensity $I(q = 0, \varphi = 0)/I(q = 0,\varphi)$ as a function of φ for the quaternary mixture PS/PDMS/PMMA/toluene at five different concentrations of PMMA. The continuous curves are the theoretical predictions and the symbols represent the data. The insert represent the variation of the diffusion coefficient D_I showing that Rouse model is good and $D_I \approx I(q = 0,\varphi = 0)/I(q = 0,\varphi)$.

3.5. *d-PS/PS/PVME*

As pointed out earlier, one of the first applications of the ZAC in polymer mixtures was due to Williams *et al.*,[16] Akcasu *et al.*[17] and King *et al.*[18] and was referred to as the "high concentration method". This method shows that, provided deuteration effects on chain conformations and interactions could be neglected, one could extract the single chain form factor or radius of gyration by performing small angle neutron scattering measurements without having to extrapolate to the zero concentration limit.

First, let us consider a solution of deuterated and ordinary polymers having degrees of polymerization N_d and N_h and concentrations c_d and c_h, respectively. In general, the coherent neutron scattering intensity $I(q)$, or the differential neutron cross section $d\Sigma(q)/d\Omega$ can be written in terms of the partial structure factors as:

$$I(q) = \upsilon_d^2 S_{dd}(q) + \upsilon_h^2 S_{hh}(q) + 2\upsilon_d\upsilon_h S_d h(q) + 2\upsilon_d\upsilon_s S_{ds}(q) + 2\upsilon_h\upsilon_s S_{hs}(q) + \upsilon_s^2 S_{ss}(q), \tag{122}$$

where υ_d, υ_h and υ_s are the scattering lengths per unit volume. Assuming that the mixture is incompressible yields:

$$S_{ss}(q) = -S_{sh}(q) - S_{dh}(q) \tag{123a}$$

$$S_{hs}(q) = -S_{hh}(q) - S_{hd}(q) \tag{123b}$$

$$S_{ds}(q) = -S_{dd}(q) - S_{hd}(q). \tag{123c}$$

Substituting these expressions into eqn (122) and using $S_{dh} = S_{hd}$ yields:

$$I(q) = (v_d - v_s)^2 S_{dd}(q) + (v_h - v_s)^2 S_{hh}(q) + 2(v_d - v_s)(v_h - v_s) S_{dh}(q). \tag{124}$$

The partial structure factor can be split into single chains $P(q)$ and interchains $Q(q)$ parts:

$$S_{dd}(q) = N_d \varphi_d [P_d(q) + \varphi_d Q_{dd}(q)] \tag{125a}$$

$$S_{hh}(q) = N_h \varphi_h [P_h(q) + \varphi_h Q_{hh}(q)] \tag{125b}$$

$$S_{hd}(q) = [N_d \varphi_d N_h \varphi_h]^{1/2} Q_{hd}(q). \tag{125c}$$

The high concentration method assumes that deuteration does not change chain conformations and interactions:

$$P(q) = P_d(q) = P_h(q)$$

$$Q_{dd}(q) = Q_{hh}(q) = Q_{hd}(q).$$

Introducing the structure factor

$$S(q) = P(q) + \varphi Q(q) \tag{126}$$

one can write the scattering intensity as:

$$I(q) = [\, < v^2 > - < v^2 >]\, N \phi P(q) + < v^2 > N \phi S(q) \tag{127}$$

where $N_h = N_d = N$, $\phi = \varphi_d + \varphi_h$ and the average contrast factors are:

$$< v > = (v_d - v_s)\varphi_d/\phi + (v_h - v_s)\varphi_h/\phi,$$

$$< v^2 > = (v_d - v_s)^2\, \varphi_d/\phi + (v_h - v_s)^2 \varphi_h/\phi.$$

Equation (127) can be written as:

$$I(q) = [v_d - v_h]^2 (\varphi_d \varphi_h/\phi^2) P(q) + < v >^2 N \phi S(q). \tag{128}$$

This shows that the form factor $P(q)$ and the structure factor $S(q)$ can be obtained by performing two measurements where φ_d/φ_h is varied keeping $\phi = \varphi_d + \varphi_h$ constant. The conditions for the high concentration method are similar to those of the ZAC when applied to an isotropic polymer mixture in solution. In practice, it is preferable to use high concentration in order to increase the signal-to-noise ratio and therefore minimizing counting time. In principle, this method can also be applied to semi-dilute and eventually to dilute solutions making the Zimm plot analysis less attractive. It also applies to polymers with more complicated architectures and to deuterated/ordinary polymers in non-solvent matrices such as polymer blends or networks provided that changing the deuterated fractions does not result in a change of the homogeneous nature of the mixture. Consider for example the case of a mixture of d-PS/PS/PVME on which small angle neutron scattering measurements were made in the following conditions:

$M_{d\text{-}PS} = 1.95 \times 10^5$ g/mole
$M_{PS} = 1.9 \times 10^5$ g/mole
$M_{PVME} = 1.59 \times 10^5$ g/mole.

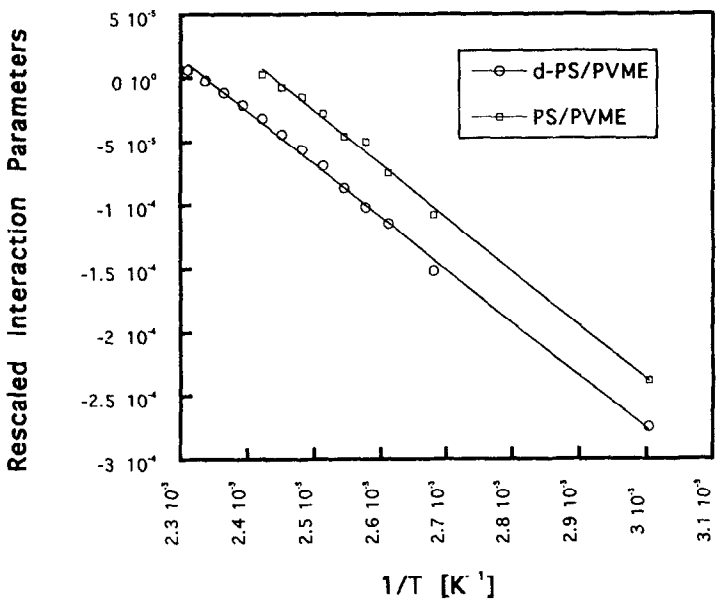

Fig. 10. The variation of the interaction parameter χ_{ab} for d-PS/PVME and PS/PVME as a function of $1/T$. These data are obtained using SANS and Flory–Huggins model.[4]

These samples were considered in small angle neutron scattering experiments and are characterized by the following volume fractions:

Sample 1:	d-PS/PS/PVME	48.4%/0%/51.6%
Sample 2:	d-PS/PS/PVME	36%/12.9%/51.1%
Sample 3:	d-PS/PS/PVME	23.8%/25.6%/50.6%

Figure 10 shows the variations of the Flory–Huggins interaction parameter between deuterated and ordinary species as a function of $1/T$ for two of these samples. These data are obtained by using the standard Flory–Huggins model. Figure 11 displays the three parts of the structure factors: $P(q)$, $Q(q)$ and $S(q)$ as extracted using the high concentration method or the ZAC condition: one notes a slight difference between the structure factors extracted from different pairs of samples because the conditions imposed for the validity of the high concentration method are not strictly satisfied. Furthermore, one may expect a slight deviation due to the fact that the assumptions of incompressibility of the mixture may not be rigorous. These aspects are discussed in more detail elsewhere.[4]

3.6. *d–PDMS/PDMS/D-toluene/toluene*

Various experiments using neutron scattering on mixtures of deuterated and ordinary polymers in mixtures of deuterated and ordinary solvents were reported under the ZAC. One of the objectives was to estimate the interaction parameter between deuterated and ordinary species χ_{hd} which, although small, could lead to significant effects in some cases. Another reason for examinining mixtures of deuterated and ordinary species is to see whether the parameter χ_{hd} has a comparable value with the pure blend when the volume fraction of

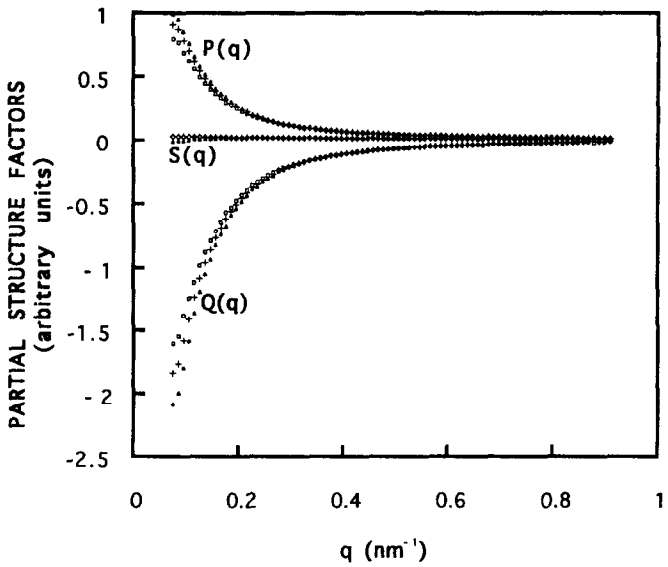

Fig. 11. The variations of the form factor $P(q)$, the structure factor $S(q)$ and the inter-chain correlation function $Q(q)$ for deuterated and ordinary mixtures of PS and PVME in the ZAC or high concentration method.[4]

solvent is zero. As an example, from the data of ordinary and deuterated PDMS in toluene,[85] it was possible to extract an interaction parameter χ_{hd} ranging between 0.2 and 0.3% which is somewhat smaller than the value characterizing pure blends. Csiba *et al.*[86] performed static and dynamic neutron scattering measurements on mixtures of d-PDMS/PDMS/d-toluene/ toluene under the ZAC. The neutron scattering experiments were also used on binary mixtures of PDMS/d-toluene under similar conditions. A number of interesting observations were made. For the quaternary mixture of deuterated and ordinary PDMS and toluene under the ZAC, it was found that the scattered intensity was proportional to the single chain form factor $P(q)$. This is an interesting system since it gives a direct access to the chain conformations and sizes. The scattered intensity for the binary system PDMS/d-toluene in the same concentration range (semi-dilute) follows the Ornstein–Zernicke equation which allows for the determination of the static correlation length ξ. Two major quantities describing the size of the polymers and the range of their composition fluctuations are deduced from such experiments. The dynamic scattering measurements give complementary information regarding the hydrodynamic size of the chains and the range of hydrodynamic screening. The neutron scattering data for the quaternary mixture under the ZAC shows that the autocorrelation function is proportional to the single chain dynamic structure factor $S(q,t)$. A fit of the neutron spin echo data with the calculated expression of Dubois–Violette and de Gennes[52] including hydrodynamic interaction indicated a good agreement. The relaxation frequency which is extracted from this fit corresponds to the motion of a single chain in the presence of hydrodynamic interaction. In the low range of q, this frequency is proportional to q^2 and the proportionality constant yields the diffusion coefficient in the Zimm model $D_s \sim N^{-0.5}$. The result can be used to measure the hydrodynamic radius R_h using the definition:

$$D_s = K_B T / 6\pi\eta R_h.$$

As q increases, there is a deviation from the q^2 behavior due to the internal relaxation modes of the chain. One finds $\Gamma(q) \sim q^3$ indicating that hydrodynamic interactions are important. Therefore, neutron spin echo measurements on PDMS and toluene mixtures under the ZAC are useful in extracting the properties of single chains in addition to χ_{hd}. It allows for the investigation of internal dynamics of the chain by looking at the modes of relaxation in the high q range. The measurement of the auto-correlation function for the mixture of PDMS and toluene mixtures showed a single decay function. The relaxation frequency of this mode $\Gamma(q)$ presents a crossover at a wavelength $1/q^*$ which is identified as the hydrodynamic correlation length ξ_h. For $q < q^* = \xi_h^{-1}$, $\Gamma(q)$ is proportional to q^2 and the proportionality constant yields the cooperative diffusion coefficient. For $q > q^*$, $\Gamma(q)$ scales as q^3 describing the internal dynamics of the chain. The crossover q^* between the q^2 and q^3 behaviors was determined quite accurately[86] and the hydrodynamic correlation length $q^* = \xi_h^{-1}$ was deduced. Similar investigations were made by Lapp *et al.*[87] on crosslinked networks of PDMS in toluene solutions using the neutron spin echo technique. However the latter experiments were not performed under the ZAC and will not be discussed here.

3.7. *Diblock copolymers of d-PS–PS/d-toluene/toluene*

Diblock copolymers in solution were also investigated under the ZAC. Both static scattering properties and dynamic properties using the spin echo technique were investigated as a function of the wavevector q and the polymer concentration c. The first study was reported by Duval *et al.*[88] who considered the static scattering from a symmetrical diblock d-PS–PS in a mixture of H_2O and D_2O fulfilling the ZAC. The static intensity was measured for several concentrations in the semi dilute range where the concentration c was roughly between c^* and $10c^*$. Within the experimental inaccuracies, all of the curves were the same and fit quite well with the simple theoretical function $P_{1/2} - P$ as indicated earlier for the case of a 50/50 diblock copolymer. In order to include the effect of small departure from the symmetry conditions and the polydispersity of the samples, Duval *et al.*[88] used, instead of $P_{1/2} - P$, the more general expression:

$$P_a + P_b - 2P_{ab} + v\varphi N(P_a P_b - P_{ab}^2)/\{1 + v\varphi N[f^2 P_a + (1-f)^2 P_b + 2f(1-f)P_{ab}]\}$$

where the subscripts a and b refer to the d-PS and PS blocks, $v\varphi N = 2A_2 Mc$ with $A_2 = 1.2 \times 10^{-3}$ cm^{3}g^{-1}mole^{-1}, and $M^w = 10\,800$ gmole^{-1}. The form factors were calculated using the standard Zimm–Schultz distribution function. The results are shown in Fig. 12 where the symbols represent the data for different concentrations and the continuous lines are theoretical predictions.

Borsali *et al.* and Duval *et al.*[91] performed NSE and quasielastic light scattering on different types of diblock copolymers in solvents.[89–91] For example, Borsali *et al.*[89] performed NSE scattering measurements on the same copolymer at a single concentration $c = 0.34$ g/cc which is roughly $3c^*$. The purpose of this preliminary study was to test whether one could observe the structural copolymer mode predicted by the RPA theory. To our knowledge, this work was the first to report the existence of the structural mode in the dynamics of block copolymers. Consistent with the theory, the intermediate scattering function was found to decay following a single exponential and the relaxation frequency Γ_I was identified with the structural mode.

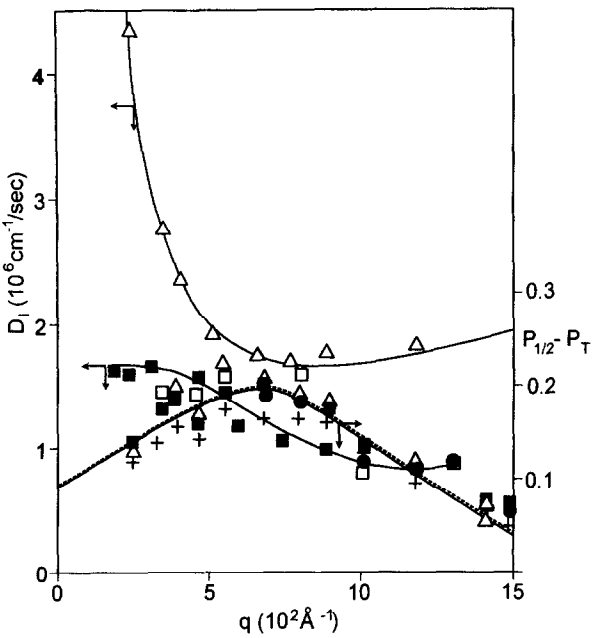

Fig. 12. The variations of the diffusion coefficient and the static scattering intensity as a function of q for a diblock copolymer d-PS–PS in toluene at different concentrations.[88,89,91]

Borsali *et al.*[89] also performed NSE measurements on the mixture of deuterated and ordinary homopolymers corresponding to the same conditions. Comparison of the copolymer and the homopolymer data showed a substantial difference that becomes more important as q decreases to zero. Whereas the normalized relaxation frequency Γ_I/q^2 increases substantially for the copolymer as q decreases to zero, the corresponding quantity for the homopolymer goes to a constant giving the diffusion coefficient D_I. This was predicted before by Akcasu *et al.*[42] and Benmouna *et al.*[92] who showed that the frequency tends to a constant as q goes to zero for the copolymer:

$$\Gamma_I = q^2 D_I/[P_{1/2}(q) - P(q)] \rightarrow 6Rg^{-2}D_I[1 + 3q^2Rg^2/8],$$

whereas for the corresponding homopolymer, one has:

$$\Gamma_I = q^2 D_I/P(q) \rightarrow q^2 D_I[1 + q^2Rg^2/3].$$

A more detailed investigation of the same copolymer was performed later for several concentrations by Duval *et al.*[91] using NSE. The time evolution of the dynamic scattering function was analyzed using the theoretical equation:

$$S(q,t)/S(q) = [(\upsilon_d - \upsilon_h)/2]^2\{P_{1/2} - P_T\}/\{1 - \chi_{hd}\varphi N(P_{1/2} - P_T)/2\}e^{-\Gamma_I t}$$

$$+ [(\upsilon_d + \upsilon_h)/2 - \upsilon_s]^2\{P_T/(1 + (\nu + \chi_{hd}/2)\varphi N P_T)\}e^{-\Gamma_C t}. \quad (129)$$

In writing this result, we did not set the smallness parameter χ_{hd} to zero to have a more general result. In the ZAC, one has $[(\upsilon_d + \upsilon_h)/2 - \upsilon_s] = 0$ and the second term on the RHS

vanishes. This means that $S(q,t)$ decays following a single exponential corresponding to the structural mode of the copolymer. As the concentration increases, both the intercept of $\Gamma_I(q = 0)$ and the slope of Γ_I/q^2 decrease. The intercept with the $q = 0$ axis is inversely proportional to the friction coefficient ζ. As expected, the data show that ζ increases with concentration. On the other hand, the generalized q dependent diffusion coefficient $D_I(q,c) = \Gamma_I/q^2$ is found to decrease with concentration consistent with the theoretical prediction. Furthermore, one observes that the generalized mobility:

$$k_B T \mu(q,c) = D_I[P_{1/2}(q) - P(q)]$$

increases as q decreases consistent with the data of $\Gamma_I(q)$. Both the latter quantity and $\mu(q,c)$ shift to higher values as the concentration increases. Some of these features are illustrated in Fig. 12 which represents the variation of D_I as a function of q for different concentrations. The normalized structure factor is also represented for one concentration along with the curve giving the theoretical prediction $P_{1/2}(q) - P(q)$. It was mentioned earlier that the normalized scattering intensity remains approximately the same in the concentration range covered in these experiments. The fact that D_I does not correspond to $1/[P_{1/2}(q) - P(q)]$ means that the mobility $\mu(q,c)$ is function of q which is a signature for the strong effects of hydrodynamic interactions.

3.8. *Diblock copolymer PS-PI in DOP*

T. Hashimoto *et al.*[35] performed small angle X-ray scattering experiments on symmetrical dibloc copolymers of PS-polyisoprene (PI) in dioctylphthalate (DOP). Their purpose was to study microdomain structures that are formed due to the spatial fluctuations in A–B diblocks as a function of the degree of polymerization N and the temperature T. Two molecular weights were considered ($M \approx 3 \times 10^4$ and 10^5). In the weak segregation limit where T is below T_c and the concentration c is below c_K, they observed that the system shows alternating microdomains with a period $D = 2\pi/q_m$, where q_m is the position of the first maximum in the scattering curve. The data were originally analyzed using a pseudo-binary model based upon the extension of the formula derived by Leibler in the case of pure diblock copolymers AB. This extension was made by replacing the interaction parameter in Leibler's equation with $\chi_{eff} = \chi_{ab}\varphi$ and the contrast factor by $[(v_a - v_b)\varphi]^2$. Their normalized scattering intensity becomes:

$$I(q)/[(v_m - v_s)\varphi]^2 = N/[P_{1/2} - P] - 2\chi_{eff}N.$$

In a subsequent paper, Hashimoto and Mori[93] reconsidered the same X-ray data, analyzing them within this pseudo-binary assumption and the more general result given in eqn (66). Since they investigated a symmetrical diblock PS-PI in DOP in the ZAC, it appears clear from the theoretical discussions that the two methods based on the pseudo-binary description and the method of eqn (66) are the same. It is interesting to note that the variation of $1/I(q = q_m)$ as a function of $1/T$ is linear in the upper temperature range, and as T decreases, one observes a significant deviation similar to the one reported earlier for the critical behavior of homopolymer blends. This means that the RPA should be improved for copolymers as well when T approaches the critical temperature for microphase separation.

3.9. *d-DNA/d-TMA/D_2O/H_2O and d-PSS/d-TMA/D_2O/H_2O*

The neutron scattering technique has been quite useful in the study of structural and dynamical properties of polyelectrolyte solutions.[94,95] It is a powerful technique for investigating the behavior of polyelectrolytes and shows in many aspects striking differences with their neutral counterparts. A particular example is given by the scattering peak in polyelectrolytes which is similar to the peak observed in block copolymers. The particular features of polyelectrolytes are due to the long range character of the electrostatic interactions and these interactions lead to regions of exclusion surrounding polyions which are known as correlation holes.[14] The scattering properties are extremely sensitive to the ionic strength of the solution which is controlled by the concentration of added salt. In the presence of excess salt, the cloud of counterions surrounding each polyion forms a shield to electrostatic forces. The structural properties at distances exceeding the screening length k^{-1} are similar to those of neutral polymers.

A polyelectrolyte solution is a typical example of a multicomponent mixture. In the simplest case of a single polyelectrolyte with added salt, one has four components: polyions, counterions due to the ionization of the polymer, counterions and co-ions of the added salt, and the solvent. In more complicated systems, one may have mixtures of polyanions and polycations. One could also use the deuteration technique to differentiate between the scattering of identical polyions. This technique is very useful in achieving a good characterization of the effects of electrostatic interactions. With the combined development of the small angle neutron scattering and the chemical labelling techniques, new prospects opened up for the characterization of polymer solution properties for both neutral and charged polymers. As we have pointed out earlier, one of the first experiments combining these advances for neutral and charged polymers were reported by Williams *et al.*, Nierlich *et al.*[96,97] and by King *et al.*[16–18] In the early experiments, the main purpose was to extract the form factor of a single labelled chain in a semi-dilute solution of unlabelled but identical chains. In a subsequent investigation, Nallet *et al.*[98] reported measurements of the partial structure factors of polyions and counterions using selective labelling of these species. The polyelectrolytes investigated were NaPSS and DNA, the counterion was the TMA and the solvent either ordinary water or its deuterated counterpart with the purpose of achieving the maximum contrast in each case. Hayter *et al.*[99] reported NSE studies of NaPSS with added salt.

More recently, neutron scattering experiments were found to be useful for investigating the structural properties of polyelectrolyte solutions under the ZAC.[94,95] In these experiments, one has a direct access to the charge–charge partial structure factor which is an important quantity describing the correlation between charged particles rather than between the labelled ones as it is usually the case for neutral polymers.

More recently, new neutron scattering measurements were reported by Van der Maarel *et al.*[94,95] on two different polyelectrolytes in the ZAC condition. The motivation for these measurements was to measure the various partial structure factors including the charge–charge structure factor for mixtures of polyions (deoxyribonucleic acid or DNA, sodium-polystyrene-sulfonate or Na-PSS) and counterions (tetramethylammonium or TMA). In the first paper, these authors reported neutron data from DNA chains (146 base-pairs, contour-length L = 500 Å) in the presence of TMA counterions in salt-free aqueous solutions of mixtures of D_2O and H_2O. The partial structure factors of the DNA polyion, the TMA counterion and the cross term polyion–counterion were measured. In another series of

experiments, mixtures of ordinary and deuterated water at a given composition were used to achieve the ZAC and evaluate directly the charge–charge structure factor. Similar measurements were performed on NaPSS molecules.

To analyze their data, Van der Maarel *et al.* developed a method which is entirely different from the one discussed here and we briefly outline the main steps of this method here. It is based upon the cylindrical cell model and the resolution of the Poisson–Boltzmann equation to obtain the distribution of counterions around the polyions. First, let us recall that the total scattering intensity can be written as

$$I(q)/c = (v_m - v_s)^2 S_{mm}(q) + (v_c - v_s)^2 S_{cc}(q) + 2(v_m - v_s)(v_c - v_s) S_{mc}(q)$$

where the subscripts m, c and s stand for monomer, counterion and solvent, respectively. The DNA or the NaPSS molecules are modelled as charged rods with length L and radius r_p. Each molecule is assumed to occupy a neutral coaxial cell of length L and radius r_{cell}. The latter depends on the concentration as $c = 1/[4\pi r_{cell}^2 \sigma]$, σ being the size of a monomer along the z-axis, i.e. $\sigma = L/N$. The distance of closest approach of the counterion to the DNA molecule is r_c which should be distinguished from the radius r_p of the polymer. The monomer concentration at a distance r from the central axis denoted $c_m(r)$ is assumed to be a constant $c_m = 1/[4\pi r_p^2 \sigma]$ for $0 < r < r_p$ and zero for $r > r_p$. The concentration of counterions in the radial direction $c_c(r)$ is obtained from the resolution of the Poisson–Boltzmann equation in cylindrical coordinates which can be made analytically. However, in this model, a severe assumption is made which consists of neglecting the correlations between different cells. Each cell is supposed to be free and experiences no interferences with its neighbors. The partial structure factors $S_{ij}(q)$ are calculated using the definition:

$$S_{ij}(q) = < c_i(q) c_j^*(q) >; \quad i = m, c$$

with

$$c_i(q) = \int_{V_{cell}} d^3 r e^{i\mathbf{q}.\mathbf{r}} c_i(r).$$

V_{cell} is the volume of a unit cell. The rest of the calculation consists of relatively simple manipulations of integrals in cylindrical coordinates and some of them have to be performed numerically.

For more details concerning these calculations, the reader is referred to the papers of Van der Maarel *et al.* In Fig. 13 we have provided the variation of the polyion–polyion structure factor obtained from these experiments for the case of NaPSS.[100] The symbols represent the data at two different concentrations as indicated in the figure caption. The dotted lines are obtained from the cylindrical cell model developed by Van der Maarel *et al.* which shows a good agreement only in the high q range above the location of the scattering peak. The poor agreement in the lower q range is probably due to the effects of inter-polyion correlations which are neglected in this model. The continuous lines in this figure are obtained from another model which was introduced in the first part of this paper. It is based on the RPA supplemented with a renormalized excluded volume parameter which is the addition of the bare excluded volume and the long range electrostatic interaction term. This model, although crude and simple, gives a good description of the data over the whole range of qs covered in the neutron scattering experiments. This is yet another example where the RPA gives surprisingly good results although it is not expected to be valid for systems with strong correlations as in the present case with polyelectrolyte solutions.

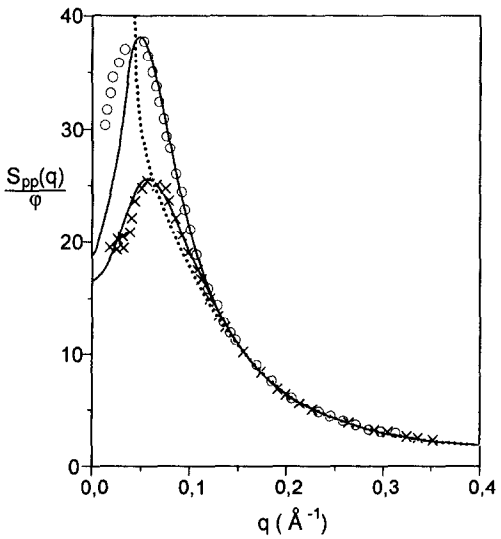

Fig. 13. The variation of the polyion–polyion structure factor $S_{pp}(q)/\varphi$ as a function of q for PSS/TMA/H_2O/D_2O mixtures and two concentrations of PSS: $\varphi = 5.98 \times 10^{-5}$ monomers/Å^3 (O) and $\varphi = 12.04 \times 10^{-5}$monomers/Å^3 ($x$). The continuous lines represent the generalized RPA and the dotted lines are predictions of the cylindrical cell model.[94,95,100]

4. CONCLUSIONS

The examples presented above indicate how a simple model based on the RPA can be useful for describing scattering data relating to the structural and dynamical properties of various polymer systems. The diversity in the systems which can be described by this method allows one to have more confidence concerning validity in obtaining a qualitative or a semi-quantitative description of a given polymer system when important quantities such as the molecular weight, the concentration, the composition and the temperature are varied. This, of course, does not mean that the mean field description is sufficient under all circumstances and that there are conditions where the RPA should be extended or at least modified to improve the description of the polymer system especially in cases where strong fluctuations take place within the system and their effects become dominant in determining the scattering behavior of the polymers. For example, in their analysis of the data of the apparent radius of gyration for the PS/PMMA/bromobenzene mixture, Kappeler *et al.*[37] had to use a renormalized form of the RPA for ternary polymer solutions to improve the fit with the experiments. To the lowest order, the renormalized theory essentially replaces the parameters of the RPA by effective quantities which are functions of concentration and molecular weight. In this case, the renormalized theory yields a result of the same structure as the classical RPA where the concentration, the degree of polymerization, the chain radius of gyration and the AB excluded volume parameter are replaced by renormalized quantities. A comparison of the data with the two RPA methods shows that the renormalized version improves the fit substantially.

We have indicated several examples where the RPA fails to describe the behavior of polymer mixtures or copolymers when one approches the critical region. In this region, it becomes clear that one should use more adequate descriptions such as the ones derived from the group renormalization theory. We have given earlier in this paper some examples

of this extension by considering the scaling behavior of the critical parameter and the critical concentration at which the system phase separates as a function of the average molecular weight of the polymers. Obviously, the mean field is unable to predict any of these scaling laws. However, it was interesting to observe that the numerical quantities obtained by extrapolation of the mean field results to the critical region yielded a reasonable agrement with the power laws predicted by the group renormalization theory.

The ZAC is a unique condition where one can have direct access to valuable information on mixtures of homopolymers, copolymers and polyelectrolyte solutions. We have presented only a few examples which demonstrate the usefulness of this method. Since its application has been made only in a few cases and relatively recenty, we expect that it will be extended to other applications and possibly to other systems. For example, one could use it to evaluate the shrinking or swelling of homopolymers or copolymers when one enters the critical region. Indeed, the ZAC condition allows one to observe directly the single chain properties (static or dynamic) even in the presence of other chains. Moreover, for the case of polyelectrolytes, one can use this method to obtain more information on the charge–charge correlations carried by polyions which to our knowledge has not yet been carried out.

ACKNOWLEDGEMENTS

M. Benmouna thanks Professor E. W. Fischer for his constant encouragement and for his kind invitation to the MPI-P in Mainz. Part of this work is based upon activities supported by the NSF under agreement 9423101.

REFERENCES

1. G.D. Wignall, *Adv. X-ray Anal.*, **36,** 355 (1993).
2. T.P. Lodge, *Mikrochim Acta*, **116,** 1 (1994).
3. J. S. Higgins and H. Benoit, *Polymers and Neutron Scattering*, Oxford Science Publications, Clarendon Press (1994).
4. B. Hammouda, *Adv. Poly. Sci.*, **106,** 89 (1992).
5. W.H. Stockmayer, *J. Chem. Phys.*, **18,** 58 (1950).
6. P. J. Flory, *Principles of Polymer Chemistry*, Cornell University Press, Ithaca (1956).
7. P. Kratochvil, J. Vorlicek, D. Strakova and Z. Tuzar, *J. Polym. Sci. Polym. Phys. Ed.*, **14,** 1561 (1976).
8. M.W.J. Van den Esker and A. Vrij, *J. Polym. Sci., Polym. Phys. Edit.*, **14,** 1943 (1976).
9. M.W.J. Van den Esker, J. Laven, A. Broeckman and A. Vrij, *J. Polym. Sci., Polym. Phys. Edit.*, **14,** 1953 (1976).
10. H. Benoit and M. Benmouna, *Macromolecules*, **17,** 535 (1984).
11. B.H. Zimm, *J. Chem. Phys.*, **16,** 1093 (1948).
12. K. F. Freed, *Renormalization Group Theory of Macromolecules*, Wiley Interscience Publications, NY (1987).
13. J. Des Cloizeaux and G. Jannink, *Polymer Solutions*, Oxford University Press (1990).
14. P. G. de Gennes, *Scaling Concepts in Polymer Physics*, Cornell University Press, Ithaca (1979).
15. T. Fukuda, M. Nagata and H. Inagaki, *Macromolecules*, **17,** 548 (1984).
16. C.E. Williams, M. Nierlich, J.P. Cotton, G. Jannink, F. Boue, M. Daoud, B. Farnoux, C. Picot, P.G. de Gennes, M. Rinaudo and M. Moan, *J. Polym. Sci., Polym. Let.*, **17,** 379 (1979).
17. Z.A. Akcasu, G.C. Summerfield, J.N. Jahshan, C.C. Han, C.Y. Kim and H. Yu, *J. Polym. Sci., Polym. Phys. Ed.*, **18,** 863 (1980).
18. J.S. King, W. Bayer, G.D. Wignall and R. Ullman, *Macromolecules*, **18,** 709 (1985).
19. P.G. de Gennes, *J. Chem Phys.*, **72,** 4756 (1980).
20. K. Binder, *J. Chem. Phys.*, **79,** 6387 (1983).

21. T. Hashimoto and H. Hasegawa, *New Funct. Mater.*, **C**, 691 (1993).
22. H. Yamakawa, *Modern Theory of Polymer Solutions*, Harper and Row, NY (1971).
23. H. Tompa, *Polymer Solutions*, Butterworths, London (1956).
24. M. Doi and S. F. Edwards, *The Theory of Polymer Dynamics*, Clarendon Press, Oxford (1986).
25. M. Daoud, J.P. Cotton, B. Farnoux, G. Jannink, G. Sarma, H. Benoit, R. Dupplessix, C. Picot and P.G. de Gennes, *Macromolecules*, **8,** 804 (1975).
26. J.P. Cotton, *J. Phys. Lett.*, **41,** 231 (1980).
27. A. Lapp, C. Picot and C. Strazielle, *J. Phys. Lett.*, **46,** 1031 (1985).
28. Z.A. Akcasu, B. Hammouda, T.P. Lodge and C.C. Han, *Macromolecules*, **17,** 759 (1984).
29. Z. A. Akcasu, *Dynamic Light Scattering: The Method and Some Applications* (W. Brown, Ed.), Oxford University Press (1992).
30. M. Benmouna and W. F. Reed, *Static Light Scattering* (W. Brown, Ed.), Oxford University Press (1996).
31. C. Strazielle, M. Duval and M. Benmouna, *Macromolecules*, **27,** 4960 (1994).
32. C. Strazielle, M. Duval and M. Benmouna, *J. Polym. Sci, Part B: Polymer Physics*, **33,** 823 (1995).
33. M. Benmouna, M. Duval, C. Strazielle, I.F. Hakem and E.W. Fischer, *Macromol. Theory Simul.*, **4,** 53 (1995).
34. T. Hashimoto, K. Sasaki and H. Kawai, *Macromolecules*, **17,** 2812 (1984).
35. T. Hashimoto and K. Mori, SANS from Block-polymers in Disordered State III Concentrated Solutions and Optically Theta-Conditions, Preprint.
36. J. Seils, M. Benmouna, A. Patkowski and E.W. Fischer, *Macromolecules*, **27,** 5043 (1994).
37. C. Kappeler, L. Schafer and T. Fukuda, *Macromolecules*, **24,** 2715 (1991).
38. A. Suriban and K. Binder, *Macromolecules*, **21,** 711 (1988).
39. D. Brosetta, L. Leibler and J.F. Joanny, **20,** 1937 (1987).
40. A. Onuki and T. Hashimoto, *Macromolecules*, **22,** 879 (1989).
41. L. Schafer and C. Kappeler, *J. Phys. (Paris)*, **46,** 1853 (1985).
42. Z. Akcasu, M. Benmouna and H. Benoit, *Polymer*, **27,** 1935 (1986).
43. T.P. Lodge, *Adv. Chem. Phys.*, **79,** 1 (1990).
44. W.W. Graessley, *Adv. Polym. Sc.*, **47,** 67 (1982).
45. W.W. Greassley, *Faraday Symp. Chem. Soc.*, **18,** 7 (1983).
46. W. Brown and P. Zhou, *Macromolecules*, **22,** 4031 (1989).
47. D. Richter, B. Ewen, B. Farago and T. Wagner, *Phys. Rev. Lett.*, **62,** 2140 (1989).
48. D. Richter, B. Farago, L.J. Fetters, J.S. Huang and B. Ewen, *Macromolecules*, **23,** 1845 (1990).
49. J. D. Ferry, *Viscoelastic Properties of Polymers*, Wiley, NY (1980).
50. R. Pecora, *J. Chem. Phys.*, **43,** 1562 (1965).
51. P.G. de Gennes, *Physics*, **3,** 37 (1967).
52. E. Dubois Violette and P.G. de Gennes, *Physics*, **3,** 181 (1967).
53. Akcasu Benmouna and C.C. Han, *Polymer*, **21,** 866 (1980).
54. W. Hess and R. Klein, *J. Phys. A Math. Gen.*, **13,** L5 (1980).
55. B. Hammouda, *Macromolecules*, **26,** 4800 (1993).
56. B. Hammouda and Z.A. Akcasu, *Macromolecules*, **16,** 1852 (1983).
57. R. Borsali, T.A. Vilgis and M. Benmouna, *Macromol. Theory Simul.*, **3,** 73 (1994).
58. D. Richter, B. Ewen and K. Binder, *J. Phys. Chem.*, **88,** 6618 (1984).
59. F. Roby and J.F. Joanny, *Macromolecules*, **25,** 4612 (1992).
60. P. Stepanek, T.P. Lodge, C. Kedrowski and F.S. Bates, *J. Chem. Phys.*, **94,** 8289 (1991).
61. P. Stepanek, *Dynamic Light Scattering: The Method and Applications* (W. Brown, Ed.), Oxford University Press (1992).
62. D. Schwahn, S. Janssen and T. Springer, *J. Chem. Phys.*, **97,** 8775 (1992).
63. G. Meier and D. Schwahn, K. Mortensen and S. Janssen, **22,** 577 (1993).
64. D.W. Hair, E.K. Hobbie, J. Douglas and C.C. Han, *Phys. Rev. Lett.*, **68,** 2476 (1992).
65. G. Meier, B. Momper and E.W. Fischer, *J. Chem. Phys.*, **97,** 5884 (1992).
66. F.S. Bates, J.H. Rosedale, P. Stepanek, T.P. Lodge, G.H. Wiltzius, G.H. Frederickson and R.P. Hjelm Jr., *Phys. Rev. Let.*, **65,** 1893 (1990).
67. M. Benmouna, J. Seils, A. Patkowski, G. Meier and E.W. Fisher, *Macromolecules*, **26,** 668 (1993).

68. J. Seils, A. Patkowski and E. W. Fisher, private communication.
69. N. Miyashita, M. Okada and T. Nose, *Polymer*, **35,** 1038 (1994).
70. N. Miyashita and T. Nose, *Macromolecules*, **28,** 4433 (1995).
71. H. Yajima, D.W. Hair, A.I. Nakatani, J. Douglas and C.C. Han, *Phys. Rev. B*, **47,** 12268 (1993).
72. L. Ould-Kaddour and C. Strazielle, *Polymer*, **28,** 459 (1987).
73. L. Ould-Kaddour and C. Strazielle, *New Trends in Physics and Physical Chemistry of Polymers* (L. H. Lee, Ed.), Plenum, Canada, p. 229 (1989).
74. L. Ould-Kaddour and C. Strazielle, *Polymer*, **33,** 899 (1992).
75. J.F. Joanny, L. Leibler and R. Ball, *J. Chem. Phys.*, **81,** 4640 (1984).
76. M.A. Anisimov and S.B. Kiselev Sov. Tech. Rev., Sect. B,. *Therm. Phys.*, **3,** 1 (1992).
77. L. Giebel, R. Borsali, E.W. Fischer and M. Benmouna, *Macromolecules*, **25,** 4378 (1992).
78. L. Giebel, R. Borsali, E.W. Fischer and G. Meier, *Macromolecules*, **23,** 4054 (1990).
79. L. Giebel, M. Benmouna, R. Borsali and E.W. Fischer, *Macromolecules*, **26,** 2433 (1993).
80. M. Benmouna, E.W. Fischer, B. Ewen and M. Duval, *J. Polym. Sci.: Part B Polym. Phys. Edit.*, **30,** 1157 (1992).
81. M. Benmouna and R. Borsali, *C.R.A.S., Paris*, **314,** 759 (1992).
82. G. D. J. Phillies, *Macromolecules*, **19,** 2367 (1986).
83. R. Borsali, private communication.
84. C. H. Wang, private communication.
85. A. Lapp, M. Motin, C. Strazielle, D. Brosetta and L. Leibler, *J. Phys.*, **II 2,** 1247 (1992).
86. T. Csiba, G. Jannink, D. Durand, R. Papoular, A. Lapp, L. Auvray, F. Boue, J.P. Cotton and R. Borsali, *J. Phys.*, **II 1,** 381 (1991).
87. A. Lapp, T. Csiba, B. Farago and M. Daoud, *J. Phys.*, **II 2,** 1495 (1992).
88. M. Duval, C. Picot, M. Benmouna and H. Benoit, *J. Phys*, **49,** 1963 (1991).
89. R. Borsali, H. Benoit, J.F. Legrand, M. Duval, C. Picot, M. Benmouna and B. Farago, *Macromolecules*, **22,** 4119 (1989).
90. R. Borsali, E.W. Fischer and M. Benmouna, *Phys. Rev. A*, **43,** 5732 (1991).
91. M. Duval, C. Picot, H. Benoit, R. Borsali, M. Benmouna and C. Lartigue, *Macromolecules*, **24,** 3185 (1991).
92. M. Benmouna, H. Benoit, R. Borsali and M. Duval, *Macromolecules*, **20,** 2620 (1987).
93. T. Hashimoto and M. Mori, *Macromolecules*, **23,** 5347 (1990).
94. J.R.C. Van der Maarel, L.C.A. Groot, J.M. Mandel, W. Jesse, G. Jannink and V. Rodriguez, *J. Phys. II France*, **2,** 109 (1992).
95. J.R.C. Van der Maarel, L.C.A. Groot, J.G. Hollander, W. Jesse, M.E. Kuil, E. Leyte, L.H. Leyte-Zuiderweg and M. Mandel, *Macromolecules*, **26,** 7295 (1993).
96. M. Nierlich, F. Boue, A. Lapp and R. Oberthur, *J. Phys.*, **46,** 649 (1985).
97. M. Nierlich, C.E. Williams, F. Boue, J.P. Cotton, M. Daoud, B. Farnoux, G. Jannink, C. Picot, M. Moan, C. Wolff, M. Rinaudo and P.G. de Gennes, *J. Phys.*, **40,** 701 (1979).
98. F. Nallet, G. Jannink, J. Hayter, R. Oberthur and C. Picot, *J. Phys.*, **44,** 87 (1983).
99. J. B. Hayter, G. Jannink, F. Brochard-Wyart and P. G. de Gennes, *J. Phys. Lett.*, **41,** L-451 (1980).
100. M. Benmouna, I. F. Hakem and T. A. Vilgis, *C. R. A. S. (Paris)*, in press.